STUDY AND ANALYSIS OF HONEYCOMB CIRCULAR, SQUARE, HEXAGONAL, AND OCTAGONAL SHAPE IN WIND TUNNEL

CHAIYAKAN PRESRI
NUNNAPAS SETTHANALERT
JACOB REINIEL PUNGUITO

A THESIS REPORT SUBMITTED IN PARTIAL FULFILLMENT
OF THE REQUIREMENTS FOR THE DEGREE OF
BACHELOR OF MECHANICAL ENGINEERING
SCHOOL OF INTERNATIONAL DISCIPLINARY ENGINEERING
PROGRAMS, SCHOOL OF ENGINEERING
KING MONGKUT'S INSTITUTE OF TECHNOLOGY LADKRABANG
2023

THESIS PROJECT OF YEAR 2023
MECHANICAL ENGINEERING, SCHOOL OF INTERNATIONAL
DISCIPLINARY ENGINEERING PROGRAMS, SCHOOL OF ENGINEERING
KING MONKUT'S INSTITUTE OF TECHNOLOGY LADKRABANG

Project Title STUDY AND ANALYSIS OF HONEYCOMB CIRCULAR, SQUARE, HEXAGONAL, AND OCTAGONAL SHAPE IN WIND TUNNEL

Student Name

1. Chaiyakan Premsri Student ID 63011118
2. Nunnapas Setthanalert Student ID 63011218
3. Jacob Reiniel Panguito Student ID 63011389

Sutapat K.
_____Advisor
(Assoc.Prof.Dr. Sutapat Kwankaomeng)

STUDY AND ANALYSIS OF HONEYCOMB CIRCULAR, SQUARE, HEXAGONAL, AND OCTAGONAL SHAPE IN WIND TUNNEL

student Chaiyakan Premsri
student Nunnapas Setthanalert
student Jacob Reniel Panguito
Advisor
Academic year 2023

ABSTRACT

This report explores multiple shapes of the screen of a wind tunnel or wind filter called honeycomb. Different shapes of honeycomb provide different results. The study employs the relationship between shapes of honeycomb and turbulence intensity. The key success is to increase wind tunnel effectiveness by reducing turbulence intensity.

The finding reveals the best shape to reduce turbulence intensity which creates more ideal fluid flow and contributes to fluid simulation study and analysis. Implications for geometrical consideration and isotropy are discussed, highlighting the continuity of fluid flow from differences in shape of honeycomb. Overall, this study advances the understanding of study and analysis of honeycomb in circular, square, hexagonal, and octagonal shape in wind tunnel and offer value insight into the computational fluid dynamics(CFD).

Chaiyakan Premsri
Nunnapas Setthanalert
Jacob Reiniel Panguito

TABLE OF CONTENTS

Chapter **Page**

LIST OF TABLES

LIST OF FIGURES

LIST OF SYMBOL

Symbol	Definition	unit
C_f	Local skin friction	-
Re	Reynold's number	-
$\overline{C}_p$	Mean pressure recovery coefficient	-
P	Pressure	Pa
p_{loss}	Pressure loss	Pa
$\mathbb{V}$	Velocity	m/s
ρ	Density	kg/m^3
c	Length	m
I	Turbulence intensity	%
ú	Root-mean-square velocity	m/s
U	Mean velocity	m/s
k	Turbulence energy	J/kg
π	Pi	
r	Radius	cm
h	Height	cm

w	Width	cm
l	length	cm
s	base length	cm

CHAPTER 1

INTRODUCTION

1.1 Research Background

In the realm of aerospace engineering, this research delves into the intricate study and analysis of wind tunnel configurations as they pertain to aircraft aerodynamics. The primary objective is to discern the most optimal shape and design within wind tunnel sections, aimed at maximizing both effectiveness and efficiency in aerodynamic field testing. This investigation encompasses a multifaceted exploration, examining the intricate interplay between the geometric configuration of wind tunnels, the intensity of turbulence within, and the consequential effects on airflow, temperature dynamics, and surface interactions.

While the immediate focus remains on aircraft applications, it is imperative to recognize the broader utility of wind tunnels across various domains, including ground vehicles and other aerodynamically sensitive structures. The underlying principles of aerodynamics and fluid mechanics serve as the cornerstone, guiding the adaptation of wind tunnel designs to suit specific testing objectives, thereby facilitating informed decision-making in manufacturing processes.

Notably, within the realm of subsonic aerodynamics, the utilization of honeycomb structures assumes a pivotal role, particularly in wind tunnels characterized by low airflow velocities, typically exhibiting Mach numbers ranging from 0.4 to 0.8. These structures, strategically integrated within the wind tunnel architecture, serve to mitigate turbulence intensity, thereby enhancing the fidelity of experimental results. Remarkably, advancements in wind tunnel technology have enabled the attainment of near-zero Mach numbers within the test section, underscoring the relentless pursuit of precision and accuracy in experimental setups.

Historically, wind tunnels have served as indispensable tools in aeronautical research for well over a century, with iconic contributions such as the Wright brothers' pioneering experiments exemplifying their enduring significance. The Wright wind tunnel stands as a testament to their ingenuity, albeit its limitations in modern contexts underscore the relentless drive for innovation and refinement. Challenges such as noise pollution, inherent to legacy wind tunnel designs, underscore the imperative for continuous improvement and adaptation in line with contemporary technological standards.

Central to this research endeavor is the recognition of honeycomb-shaped designs as a potential panacea, promising a paradigm shift in wind tunnel performance by ameliorating turbulence-induced distortions. By leveraging insights gleaned from this investigation, it is envisaged that future wind tunnel designs will exhibit heightened efficacy and efficiency, thereby catalyzing advancements across diverse aerospace and engineering disciplines.

1.2 Objective

To increase the effectiveness and efficiency of the wind tunnel. There are many factors required to be considered.

1.2.1 To study the airflow in the wind tunnel

1.2.2 To study the turbulence intensity

1.2.3 To study the temperature of the surface regarding the temperature of the aircraft engine itself.

1.2.4 Importance of honeycomb design in 4 sections (circular, square, hexagonal, and octagonal section)

1.2.5 The relation between the analysis of aerodynamics and designs.

1.3 Hypothesis

The octagon honeycomb wind tunnel would be the most effective subject due to the strong structure of the honeycomb design and edges of the octagon which help in decreases in pressure loss which increase the pressure. Consequently, the air flow and turbulence would be higher as well.

1.4 Scope of study

1.4.1 Types of wind tunnel

1.4.2 Types of honeycomb structure

1.4.3 Shape of honeycomb structure

1.4.4 Principle of aerodynamics

1.4.5 Pressure distribution

1.4.6 Velocity distribution

1.4.7 Turbulence intensity distribution

1.4.8 Specific energy theory

1.4.9 Darcy-Weisbach Model

1.5 Procedure

1.5.1 Study about the type of wind tunnel used in this experiment

1.5.2 Study about the difference of structures in circular, square, hexagon, and octagon honeycomb wind tunnel

1.5.3 Study about the factors related and parameters in this experiment

1.5.4 Create a stimulation version of the experiment of four different designs

1.5.5 Analyze and compare the results of four designed honeycomb

1.5.6 Create 3D print model of four designed honeycombs

1.5.7 Test 3D print model

1.5.8 Compare the result of stimulation and 3D print models for external parameters in addition.

1.6 Expected Benefit

1.6.1 Increase the effectiveness and efficiency result in wind tunnel

1.6.2 Applying the result and design to the industry

CHAPTER 2

LITERATURE REVIEW

This research is specifically aimed to develop the effectiveness and efficiency of wind tunnels of aircraft. However, wind tunnels appeal in several industrial fields. One of the significant issues is pressure loss in the wind tunnel which affects the air flow and turbulence intensity. To improve the issue, there are many parameters considered.

One way is to design the honeycomb into a hexagonal section. Hexagonal shape is the most effective design in a modern day but what if creating an octagonal section gives more benefit. There are various researches. studying the design of it.

2.1 Type of wind tunnel

There are many ways to classify wind tunnel regarding style, output, configuration, and speed

2.1.1 Speed

Wind tunnels can be classified by the speed of air passing through the test section relative to the speed of sound which can be divided into four types which are subsonic, transonic, supersonic, and hypersonic regarding Mach number as a classification.

2.1.2 Configurations

Open-loop and closed-loop configurations are the most common wind tunnels in the industrial field for experimental testing.

2.1.2.1 Open-loop wind tunnel

Open-loop type has open end on both sides and gathers air from the environment, when the air passes through the end of the testing section it is recirculated

through the room and enters the testing section again. Open-loop wind tunnel has lower cost construction and superior design for propulsion and smoke visualization. There is no accumulation of exhaust product in an open tunnel. There are many disadvantages as well such as poor flow quality in the testing section, high operation cost, and noisy operation. The Wright Brother wind tunnel[1] is also an open-loop system. The utilization of a basic wind tunnel by the Wright brothers in 1901 for investigating the impact of airflow on different shapes during the creation of their Wright Flyer was, in certain respects, groundbreaking. Nevertheless, it becomes evident from the aforementioned information that they were merely employing the prevailing technology of that era, even though this technology had not yet become widespread in the United States.

Figure 1. Open-loop wind tunnel

2.1.2.2 Closed-loop wind tunnel

This variety of tunnel is alternatively referred to as a "Prandtl tunnel," named after the German engineer, or a "Göttingen tunnel," named after the research laboratory in Germany where it was initially employed. Many of NASA's expansive research wind tunnels are of the closed return type. Within a closed return tunnel, air is directed from the test section's exit back to the fan using a sequence of turning vanes. After exiting the fan, the air is directed back to the contraction section and then through the test section again. This

maintains a continuous circulation of air throughout the duct system of the closed return tunnel, as indicated by the arrows in the diagram. In the other primary tunnel design, the open return tunnel, air that traverses the test section is drawn from the room in which the tunnel is situated.

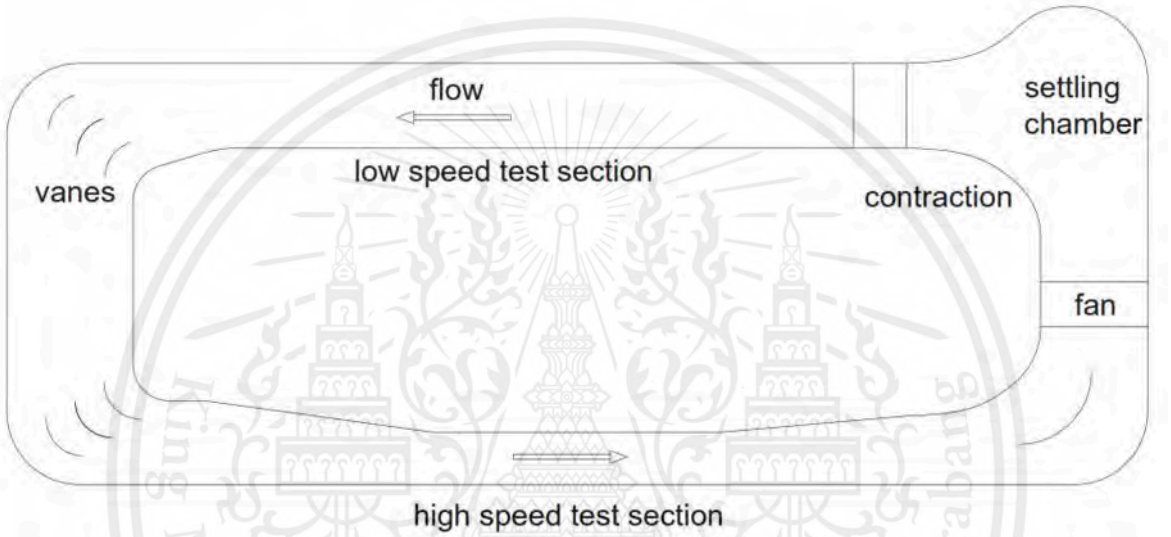

Figure 2. Closed-loop wind tunnel

Gordon and Imbabi [2] examined the potential for enhancing the design of conventional tunnel components through the utilization of CFD tests. They applied the mass and momentum equations of the Brinkman model to describe the flow of fluid through screens. The Brinkman model's momentum equation for porous media was used to represent fluid flow through screens.

Kulkarni et al. [3] investigated how honeycomb and combinations of honeycomb and screens can reduce vorticity and turbulence in a subsonic flow test section. They achieved this by solving the governing equations for subsonic flow using turbulent and porous flow models within the ANSYS-CFX CFD software.

Fadilah and Erawan [4] employed NUMECA software to simulate the impact of screens and honeycomb structures on flow quality in a wind tunnel. They used the Darcy model to represent the screen and honeycomb. These screen and honeycomb structures also find applications in thermal power systems, such as air solar systems and thermal storage systems.

Moonen et al. [3] introduced a novel approach for numerically simulating flow conditions in a closed-circuit wind tunnel. They evaluated the CFD function for wind tunnel measurement and design. Their method generally replicated wind tunnel measurements of average velocities with an error of 10% or less. In a subsequent study, the same authors [4] developed a set of six new complementary indicators for assessing the spatial flow quality in wind tunnel test sections using the previously established methodology.

2.2 Aerodynamic

In aerodynamics of the plane, wind turbine engine support in velocity distribution. The design of aerodynamics can be tested in a wind tunnel. Nearly all aircraft designs are tested in wind tunnels, in order to accurate the performance and reduce the financial risk. The aerodynamic side of wind tunnels change its performance related to the shape of the screen.

The researcher named Hudhaifa Hamzah [5] has a related research of Honeycomb in Improving Subsonic Wind Tunnel Flow Quality. Which said " Flow control is mainly achieved by controlling the separation of the boundary layer and various possible approaches have been applied experimentally to re-straighten the flow, such as

installing honeycombs and anti-turbulence screens.” meaning that the shape of the honeycomb screen has the effect of reducing the flow in wind tunnels.

Schubauer and Spangenberg [6] using screens to check the flow quality of the wide-angle diffusers. They observed that the presence of screens could have prevented or delayed the flow separation in these diffusers depending on their position. Furthermore, Honeycomb has been utilized successfully for many years as a means of straightening and directing airflow for many applications such as air conditioners, ducts, and heaters.

Each shape of the wind tunnel gives different results. Also the position of the screen can change the diffuser abilities, velocity distribution, pressure distribution, and aerodynamic analyses in the same speed of wind (air velocity).

İbrahim Göv[7] “Comparison of Hexagonal, Square and Circular sectioned Honeycomb performance in a wind tunnel.” In this study the turbulence intensity of each sectioned Honeycomb was investigated and how to minimize and improve the accuracy of the honeycomb.

Turbulence is a form of irregular flow which due to various variations result in infinite velocity. Turbulence can cause unwanted or unstable results from the experiment due to the difference in turbulence spectra. To reduce the turbulence, a screen or honeycomb was created to even out the velocity variation of flow. It can reduce a large vortex structure and therefore, reduce turbulence for the experiment to have acceptable results.

CHAPTER 3

METHODOLOGY

3.1 Hypothesis

Stimulation analysis for the purpose of measuring the pressure drop, air flow quality, turbulence intensity, and velocity of air by using the following hypothesis

- Fluid flow
- Turbulance
- Velocity of air flow
- Heat occur during the testing is neglectable

3.2 Related equation for mathematical model

Local skin friction coefficient, C_f

$$Cf = -\frac{2\omega}{Re} \tag{3-1}$$

Mean pressure recovery coefficient, $\overline{C}_p$

$$\overline{C}_p = \frac{\overline{P}_2 - \overline{P}_1}{\frac{1}{2}\mathbb{V}1^2} \tag{3-2}$$

Pressure loss p_{loss}

$$p_{loss} == (P1 - P2) + \frac{1}{2}(\varepsilon_1 \mathbb{V}_1^2 - \varepsilon_2 \mathbb{V}_2^2) \tag{3-3}$$

Where Reynold Number,

$$\mathrm{Re} = \frac{\rho V c}{\mu} \tag{3-4}$$

Turbulence intensity

$$I = \frac{\acute{u}}{U} \tag{3-5}$$

Where $\acute{u} = \sqrt{\frac{1}{3}(\acute{u}_x^2 + \acute{u}_y^2 + \acute{u}_z^2)}$ (3-6)

$$\acute{u} = \sqrt{\frac{2}{3}k} \quad (3\text{-}7)$$

And $U = \sqrt{U_x^2 + U_y^2 + U_z^2}$ (3-8)

3.3 Screen shape in Wind tunnels

Honeycomb are used to reduce the disturbance and turbulence of wind tunnels. Also help the flow effect of temperature on the surface. There are many shapes of honeycomb in wind tunnels but this thesis focuses on four types which are circular, square, hexagon, and octagonal.

3.3.1 Honeycomb circular

Circular shape in honeycomb (figure 3.3.1.1) is a honeycomb structure that is designed with a circular section shape. Each individual cell repeats and makes up the honeycomb. The circular cells provide a continuous, smooth surface.

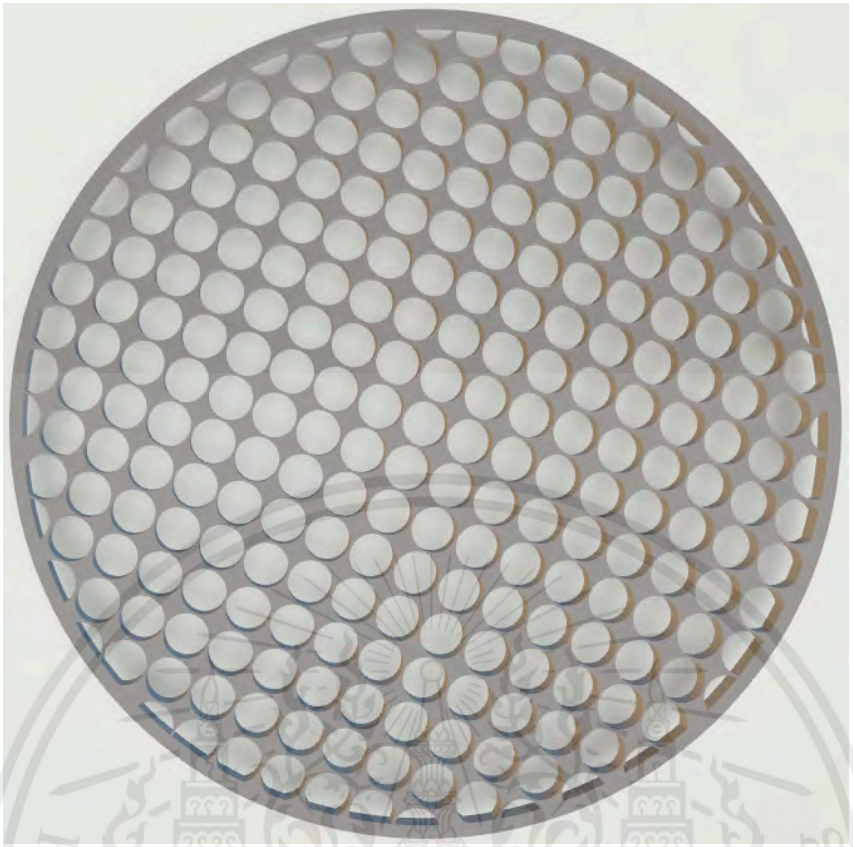

(Figure 3.3.1.1) Circular honeycomb

3.3.2 Honeycomb Square

Honeycomb square refers to a honeycomb structure with square-shaped cells. In a honeycomb square, the individual cells are arranged in a grid-like pattern, and each cell has four equal-length sides and four right angles, resulting in a square shape.

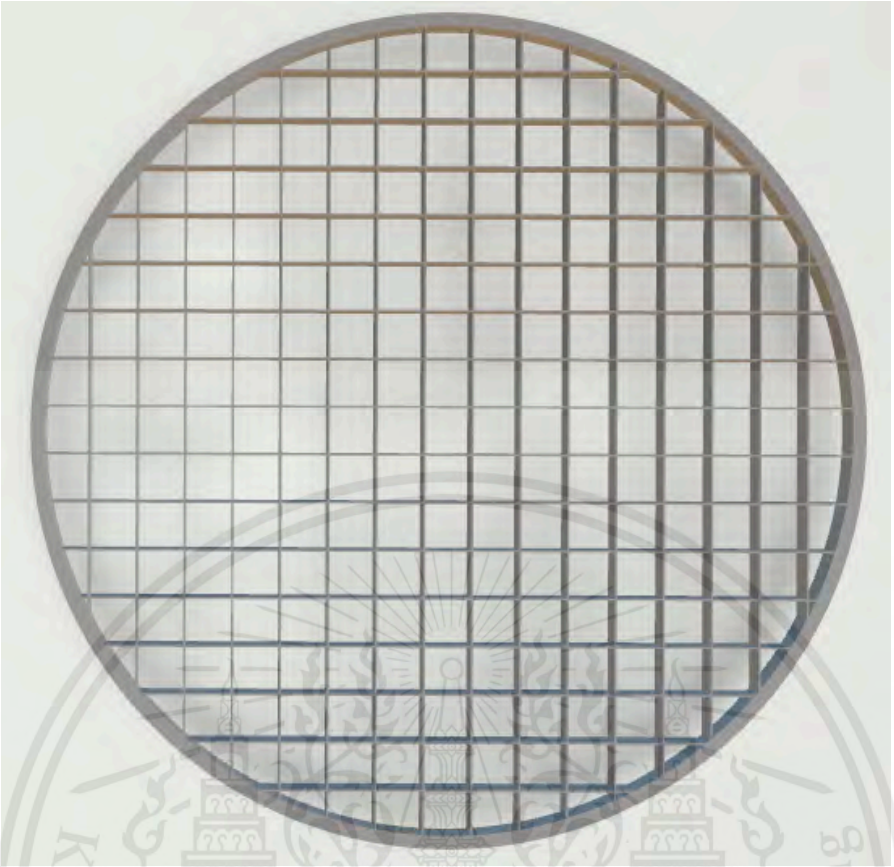

(Figure 3.3.2.1) Square honeycomb

3.3.3 Honeycomb Hexagonal

Hexagonal cell honeycomb is an original design of honeycomb. It's also the most common shape of honeycomb. The structural design is composed of hexagonal-shaped cells that are arranged closely together.

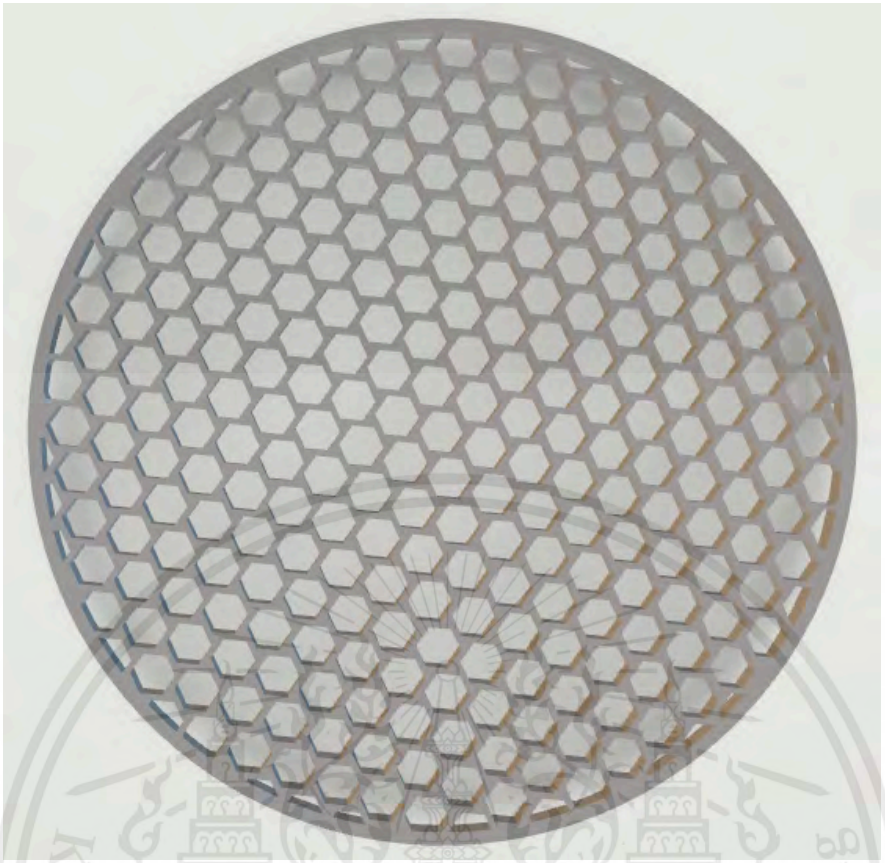

(Figure 3.3.3.1) Hexagonal honeycomb

3.3.4 Honeycomb Octagonal

Honeycomb octagonal refers to a layout or pattern in octagons, which are eight sided polygons, arranged regularly, repeating. It has a unique geometric character and can maximize the performance of honeycomb shape.

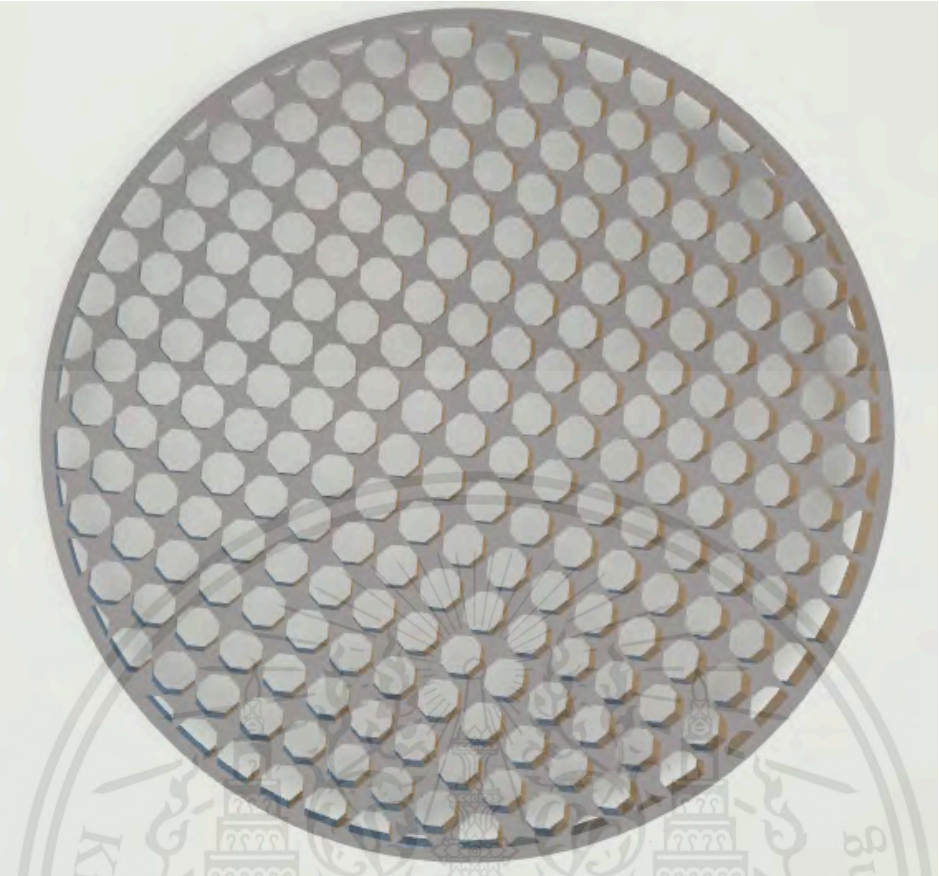

(Figure 3.3.4.1) Octagonal honeycomb

3.4 Turbulence and turbulence intensity

Turbulence is the instability of fluid which frequently has a negative impact on the outcome. It is a motion which involves velocity and pressure. In the realm of fluid dynamics, turbulence, or turbulent flow, denotes the dynamic state of a fluid marked by erratic alterations in pressure and flow velocity. This state contrasts sharply with laminar flow, a condition wherein a fluid moves in orderly, parallel layers without any significant disruption or mixing between them. Turbulence manifests as swirling eddies and vortices within the fluid, leading to complex and often unpredictable patterns of motion. These turbulent phenomena are governed by nonlinear interactions between various forces acting on the fluid, including inertia, viscosity, and external disturbances. Despite its inherently chaotic nature, turbulence plays a crucial role in numerous natural and engineering processes, influencing

phenomena ranging from atmospheric dynamics and ocean currents to the performance of aircraft and industrial machinery.

Turbulence and turbulence intensity are interconnected concepts in fluid dynamics, yet they possess distinct characteristics. Turbulence denotes the erratic and irregular movement of fluid particles, showcasing fluctuations in both velocity and pressure. This phenomenon involves the formation of swirling patterns and turbulent structures within the fluid flow. In contrast, turbulence intensity serves as a quantitative gauge of the level of turbulence within a flow field. It typically quantifies the ratio of root mean square (RMS) velocity fluctuations to the mean flow velocity, offering insights into the magnitude of turbulence relative to the overall flow velocity.

While turbulence describes the phenomenon itself, turbulence intensity provides a numerical representation of the strength or extent of turbulence within a given flow.

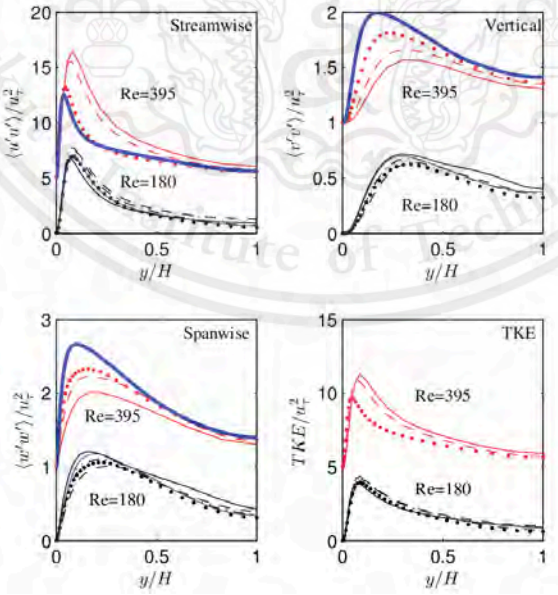

(Figure 3.4) Turbulence intensity components

3.5 Solid-fluid interaction surface and corner cells

In the realm of solid-fluid interaction surfaces, the term "corner cell" typically refers to a computational grid unit situated at the junction of solid boundaries within a computational fluid dynamics (CFD) simulation.

These cells are pivotal in accurately depicting fluid flow near solid boundaries, particularly in intricate geometries. They enable the representation of fluid flow dynamics around sharp edges, corners, or irregularities in the solid surfaces.

In numerical simulations, special treatment is often applied to corner cells to ensure precise and stable computations. Techniques like grid refinement, adaptive meshing, or specialized boundary conditions may be employed to effectively handle corner cells and mitigate numerical instabilities or inaccuracies.

Understanding and appropriately addressing corner cells are vital for achieving dependable simulations of solid-fluid interaction surfaces across diverse engineering and scientific domains, including aerodynamics, heat transfer, and fluid-structure interaction analyses.

CHAPTER 4

RESULT AND ANALYSIS

4.1 Operational plan

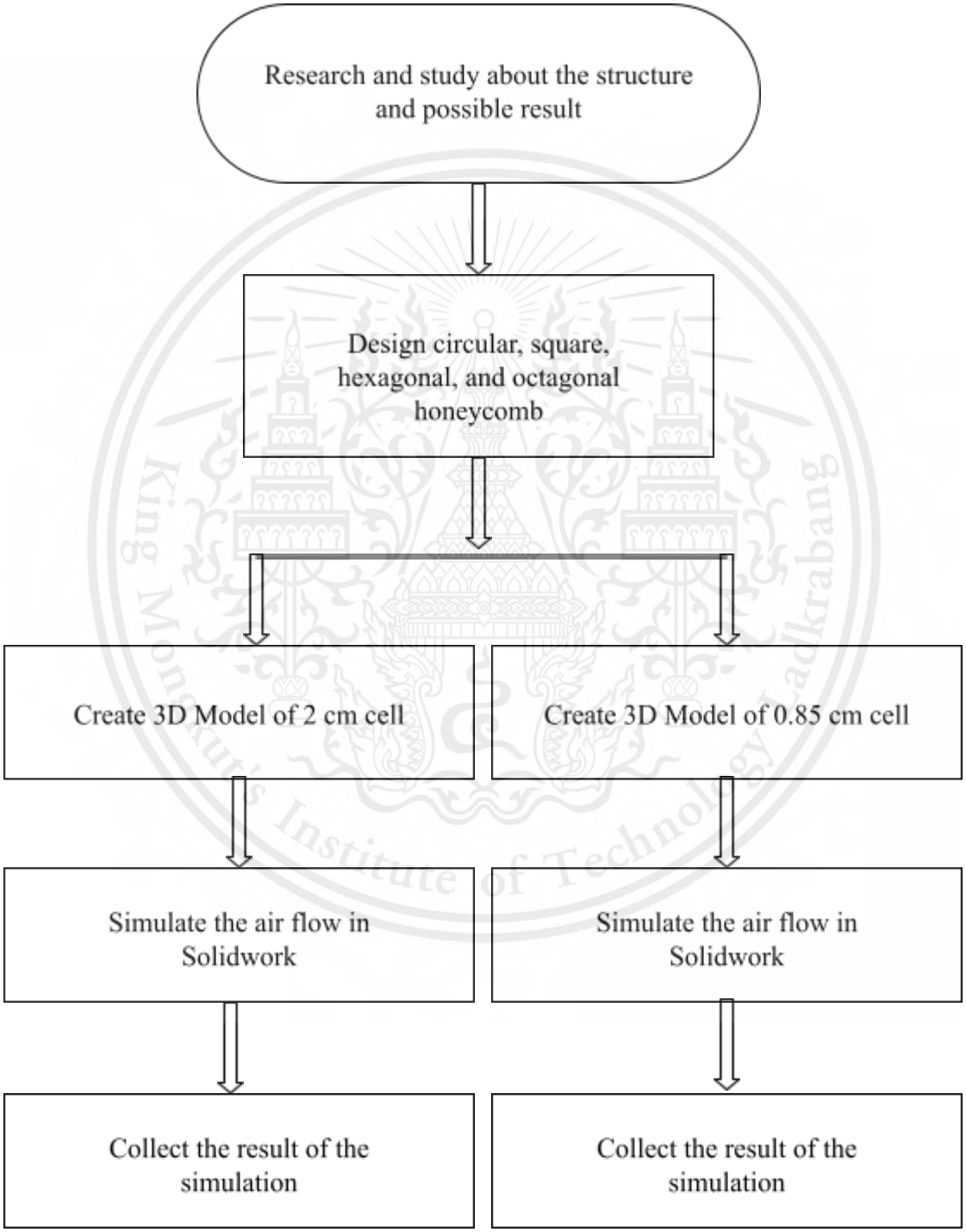

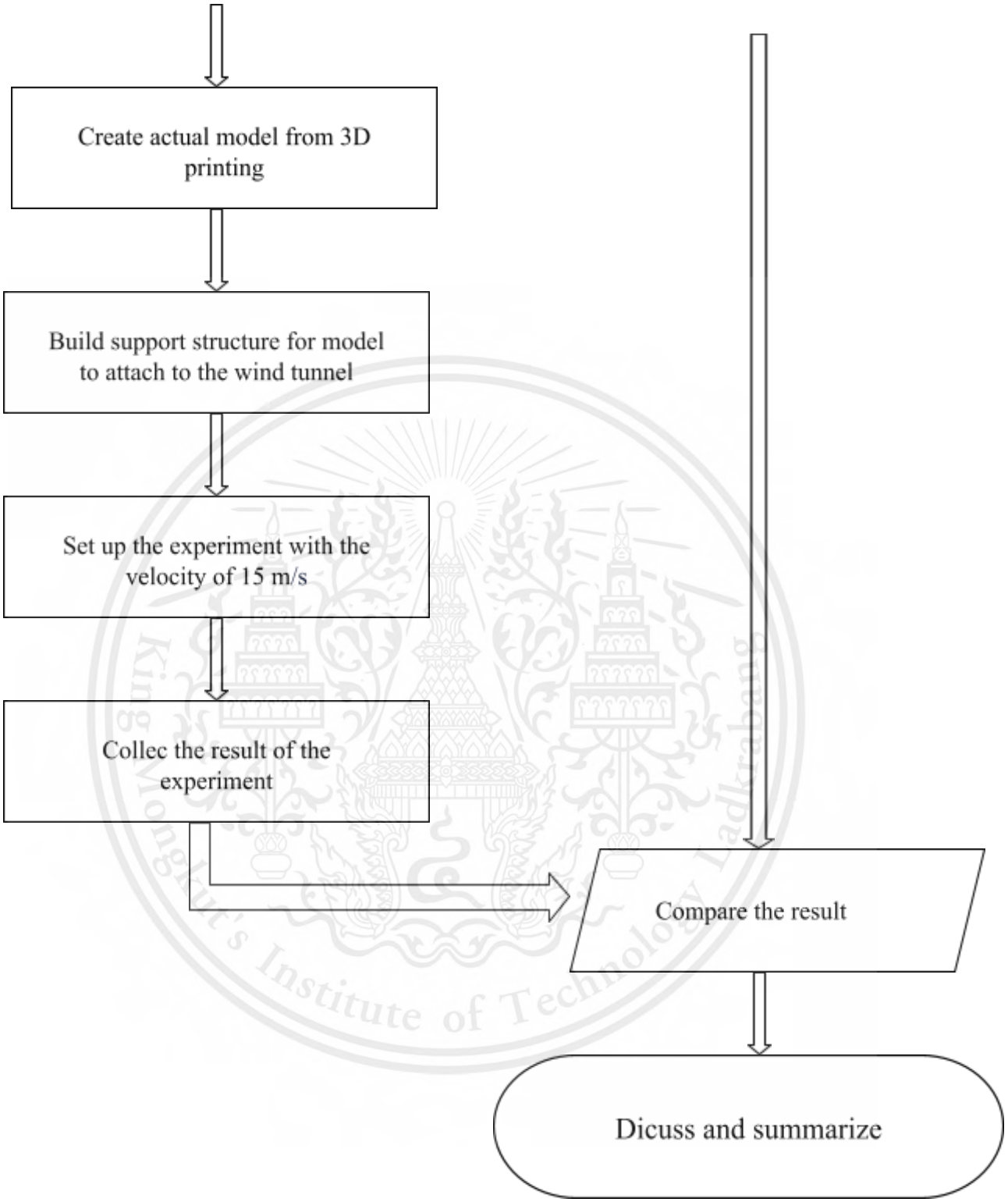

These are the processes needed to acquire in this study. By working as the following steps, the outcome will be accurate, precise, and organized. After researching and studying

the principle of the honeycomb, the next step is to design 4 different shapes of the honeycomb which are circular, square, hexagonal, and octagonal honeycomb as listed.

4.2 Model Trial 1

There are 2 experiments which are to analyze design and size. First experiment aims to create a design to find the right shape of honeycomb which supposes to reduce turbulence intensity. Second experiment aims to analyze the size of each grid for a more effective result. The result of the first design will be compared to the second experiment to analyze if the size of each grid is one of the factors for turbulence intensity reduction.

4 design models which are circular, square, hexagonal, and octagonal honeycomb are created in Fusion 360. Sizing is created based on individual longest diagonal and diameter(for circular honeycomb)

	Volume per grid (cm^3)	Outer Diameter (cm)	offset (cm)	Diameter (cm)	Long diagonal (cm)	Quantity	Distance (cm)	Angular Direction
Circular	15.71	15	0.25	2	-	9×9	7	135:45
Square	20.0	15	0.25	-	2	9×9	7	90:180
Hexagon	12.99	15	0.25	-	2	9×9	9.5	135:45
Octagon	14.14	15	0.25	-	2	9×9	9.5	135:45

Table. 1 Sizing and dimension of honeycomb

4.2.1 Circular honeycomb

The volume of cylinder per grid

$$volume = \pi r^2 h$$

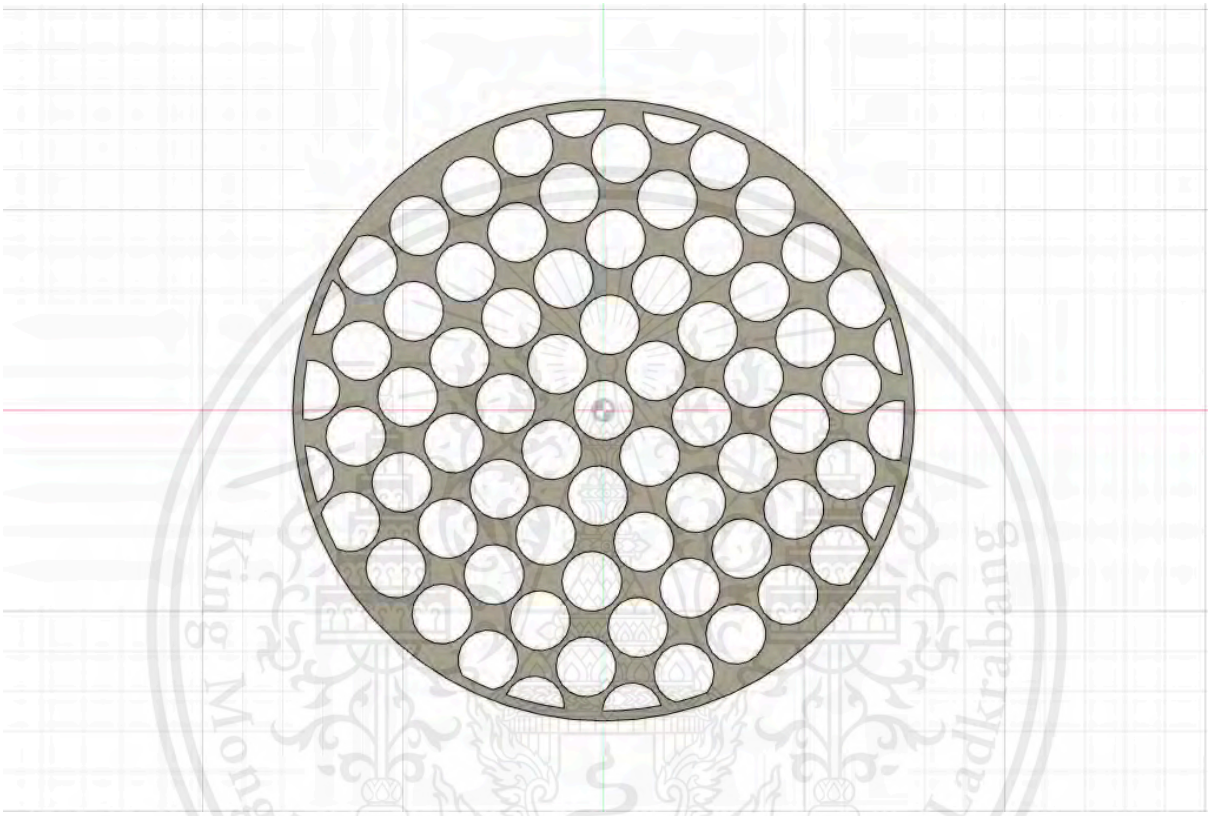

(Figure) 4.2.1 Top view perspective of circular honeycomb

(Figure) 4.2.1.1 3D Circular honeycomb model

Design process

4.2.1.1 Using Fusion 360 and select the plane of work to the bottom plane

4.2.1.2 Create a circle with a diameter of 15 cm.

4.2.1.3 Create an offset or an outer circle of 0.25 cm.

4.2.1.4 Create an inner circle with a diameter of 2 cm.

4.2.1.5 Create 2 directional lines of 135° and 45°

4.2.1.6 Select a rectangular pattern from the create section and select a circle of diameter 15 cm.

4.2.1.7 Select direction, quantity, distance and pattern to be symmetric.

4.2.1.8 Suppress the excessive circular and trim an unwanted line

4.2.1.9 Extrude the model and save as STL

4.2.2 Square honeycomb

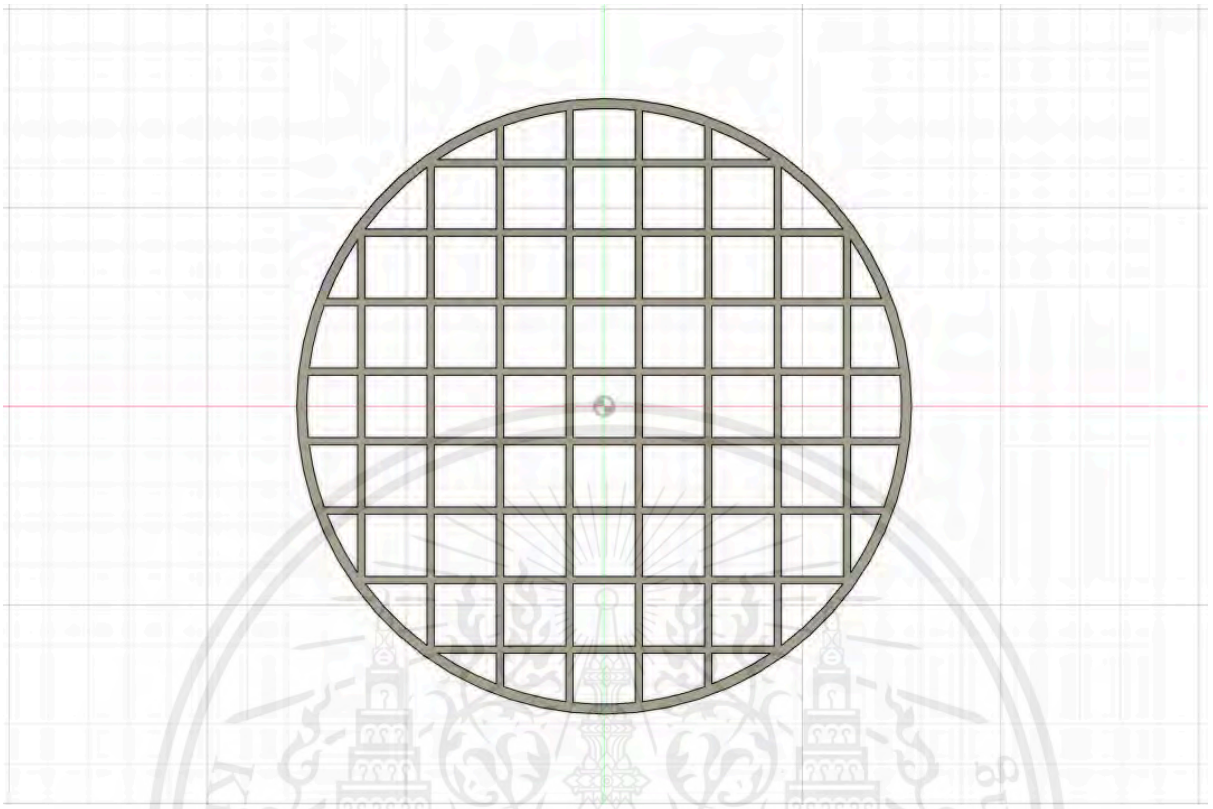

(Figure) 4.2.2 Top view perspective of square honeycomb

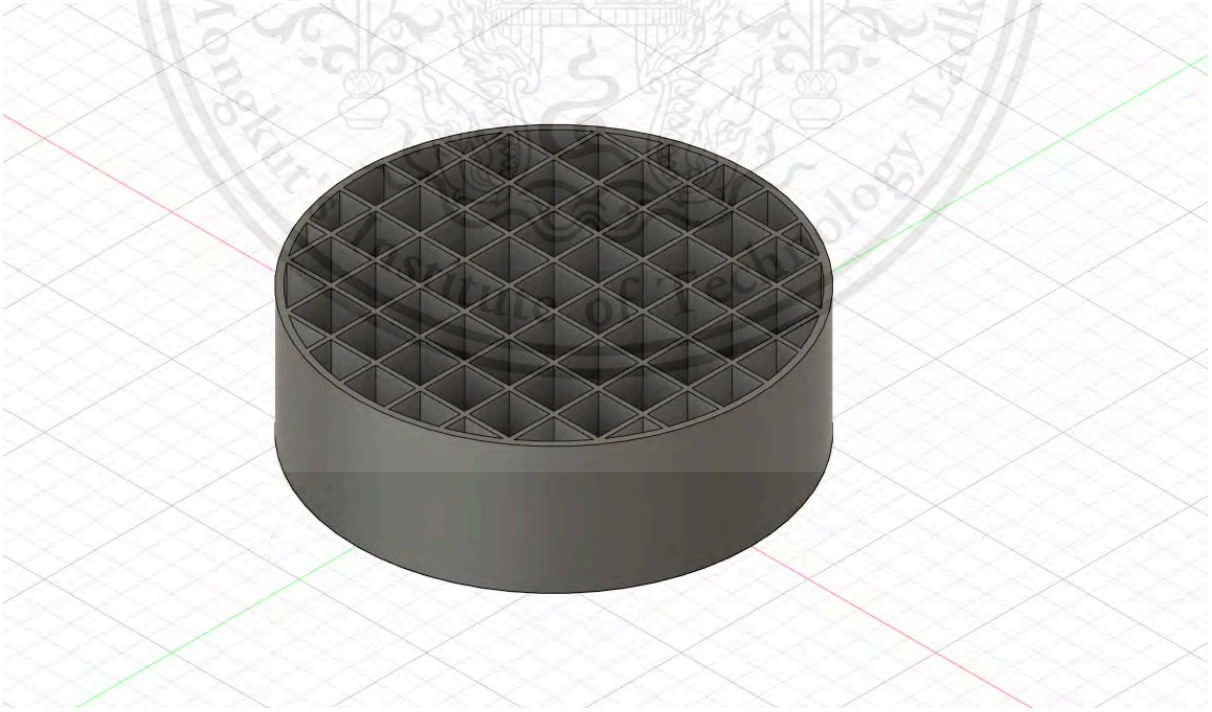

(Figure) 4.2.2.1 3D Square honeycomb model

The volume of rectangular tube per grid

$$volume = w \times l \times h$$

Design process

4.2.1.1 Using Fusion 360 and select the plane of work to the bottom plane

4.2.1.2 Create a circle with a diameter of 15 cm.

4.2.1.3 Create an offset or an outer circle of 0.25 cm.

4.2.1.4 Create a square with a width and length of 1.57 cm.

4.2.1.5 Create 2 directional lines of 180° and 90°

4.2.1.6 Select a rectangular pattern from the create section and select a circle of diameter 15 cm.

4.2.1.7 Select direction, quantity, distance and pattern to be symmetric.

4.2.1.8 Suppress the excessive circular and trim an unwanted line

4.2.1.9 Extrude the model and save as STL

4.2.3 Hexagonal honeycomb

The volume of hexagonal tube per grid

$$volume = \left[\frac{3\sqrt{3}}{2}\right] s^2 h$$

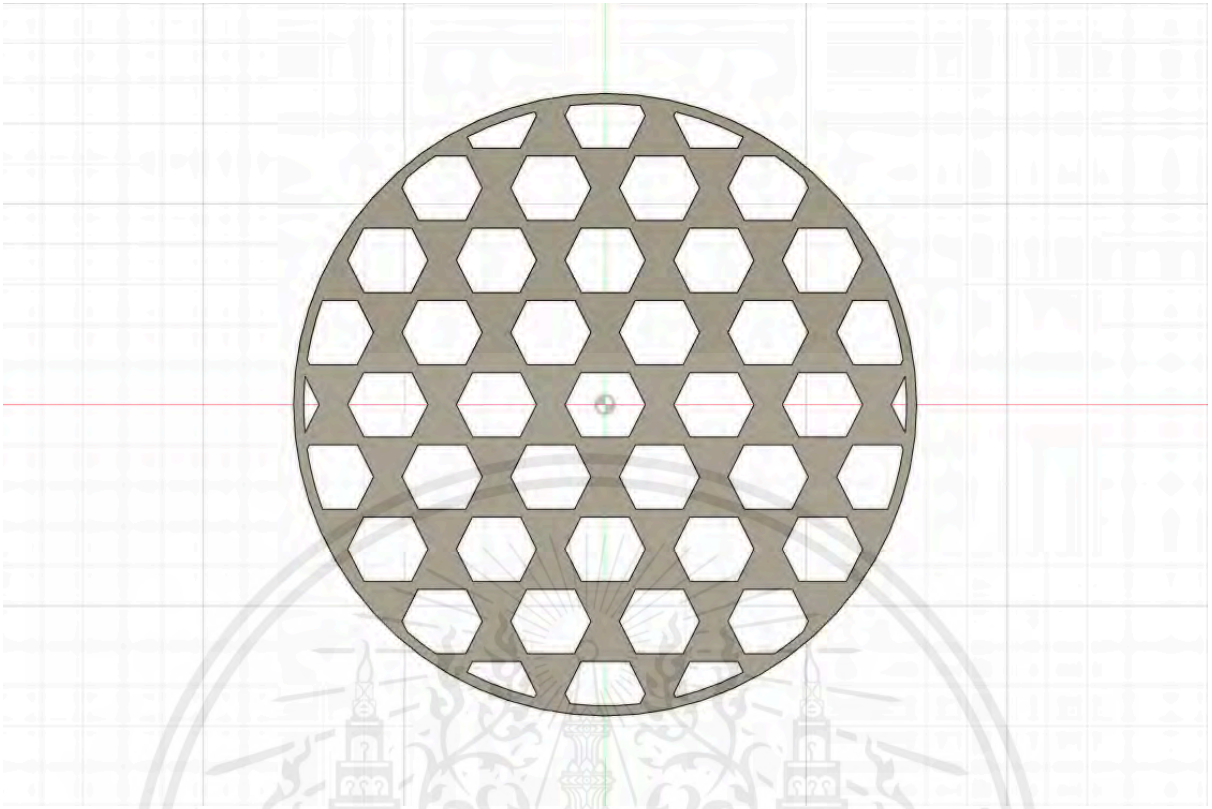

(Figure) 4.2.3 Top view perspective of hexagonal honeycomb

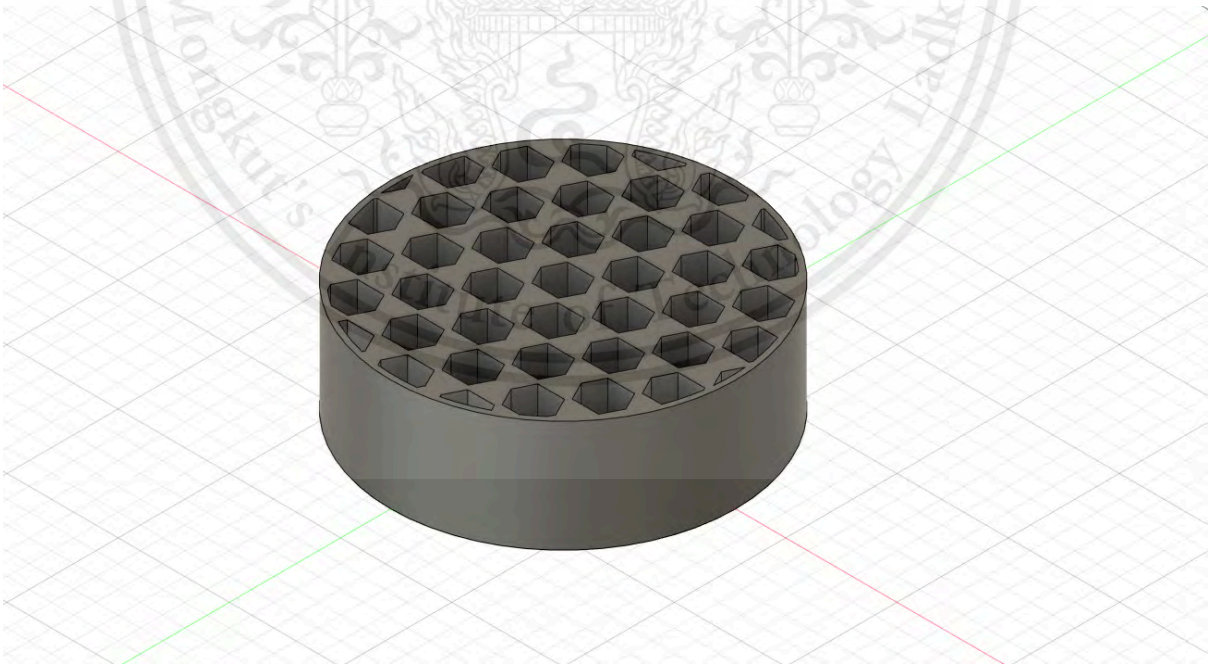

(Figure) 4.2.3.1 3D Hexagonal honeycomb model

Design process

4.2.1.1 Using Fusion 360 and select the plane of work to the bottom plane

4.2.1.2 Create a circle with a diameter of 15 cm.

4.2.1.3 Create an offset or an outer circle of 0.25 cm.

4.2.1.4 Create a hexagon with 6 equal sides of 1 cm.

4.2.1.5 Create 2 directional lines of 180° and 90°

4.2.1.6 Select a rectangular pattern from the create section and select a circle of diameter 15 cm.

4.2.1.7 Select direction, quantity, distance and pattern to be symmetric.

4.2.1.8 Suppress the excessive square and trim an unwanted line

4.2.1.9 Extrude the model and save as STL

4.2.4 Octagonal honeycomb

The volume of honeycomb per grid

$$volume = 2(1 + \sqrt{2})s^2h$$

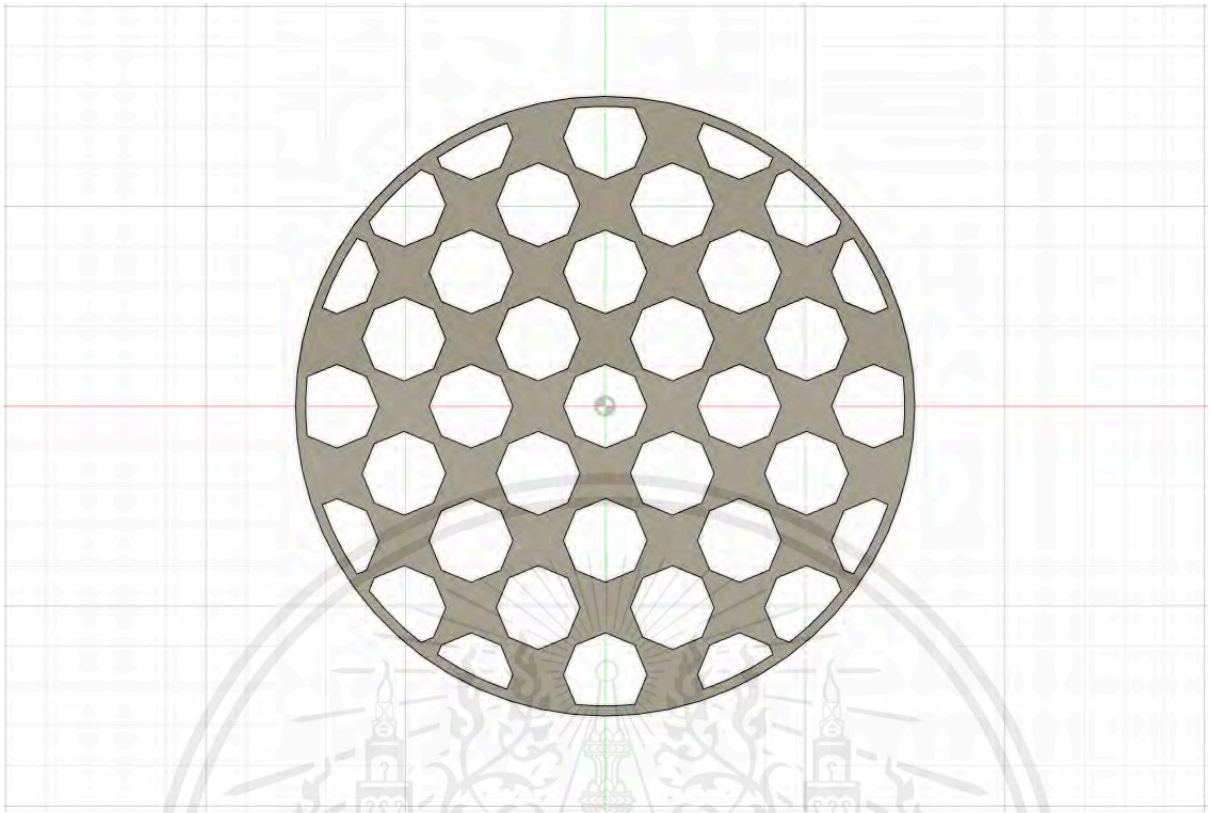

(Figure) 4.2.4 Top view perspective of Octagonal honeycomb

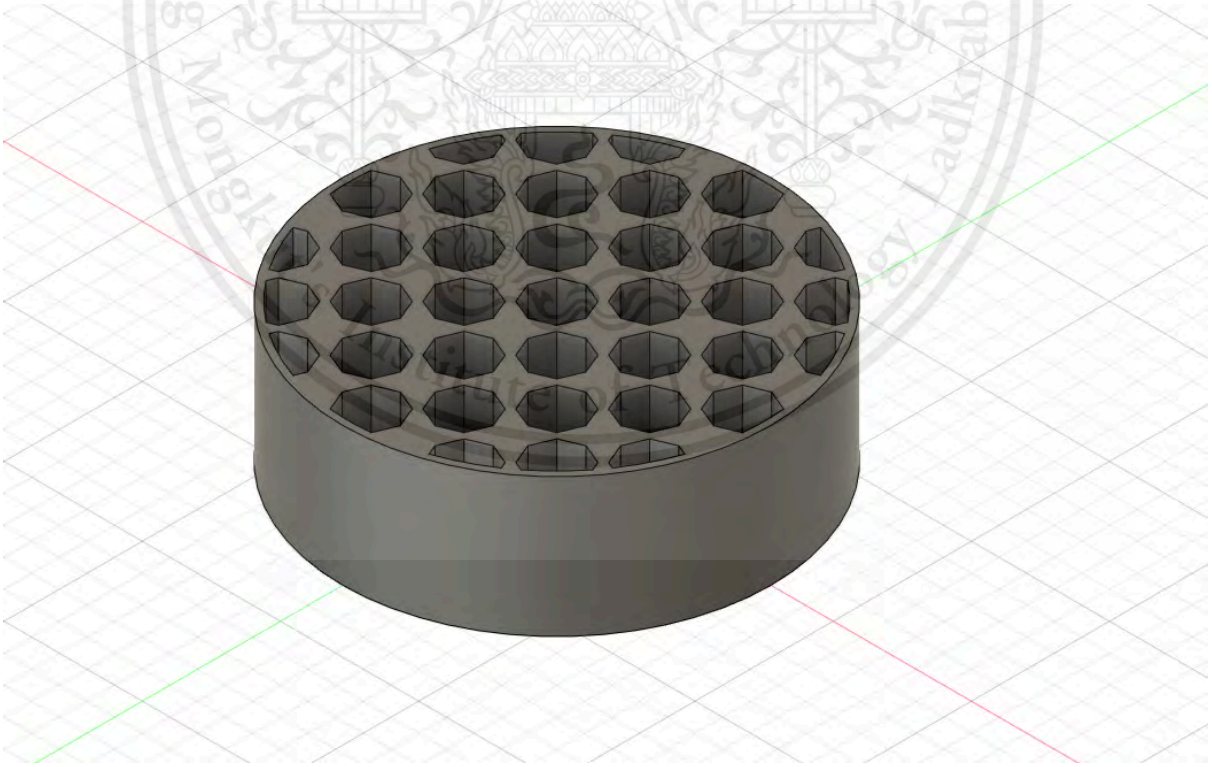

(Figure) 4.2.4.2 3D Octagonal honeycomb model

Design process

4.2.1.1 Using Fusion 360 and select the plane of work to the bottom plane

4.2.1.2 Create a circle with a diameter of 15 cm.

4.2.1.3 Create an offset or an outer circle of 0.25 cm.

4.2.1.4 Create a square with 8 equal sides of 0.77 cm.

4.2.1.5 Create 2 directional lines of 135° and 45°

4.2.1.6 Select a rectangular pattern from the create section and select a circle of diameter 15 cm.

4.2.1.7 Select direction, quantity, distance and pattern to be symmetric.

4.2.1.8 Suppress the excessive octagon and trim an unwanted line

4.2.1.9 Extrude the model and save as STL

The distance between the grid of hexagon and octogon is different from circular and square honeycomb due to the ability of 3D printing. Since a small gap cannot be modified. Therefore, the gap of hexagon and octogon is larger.

4.3 Model Trial 2

As mentioned above, the second experiment is to compare the first result. As the grid is reduced by size.

In this part, there are 4 similar designs with the smaller size as following data

	Volume per grid (cm^3)	Outer Diameter (cm)	offset (cm)	Diameter (cm)	Long diagonal (cm)	Quantity	Distance (cm)	Angular Direction
Circular	2.84	15	0.25	0.85	-	18×18	8×8	135:45
Square	3.61	15	0.25	-	0.85	18×18	8×8	90:180
Hexagon	2.35	15	0.25	-	0.85	35×35	8×8	135:45
Octagon	2.55	15	0.25	-	0.85	35×35	8×8	135:45

Table. 2 Sizing and dimension of Trial 2

4.3.1 Circular honeycomb

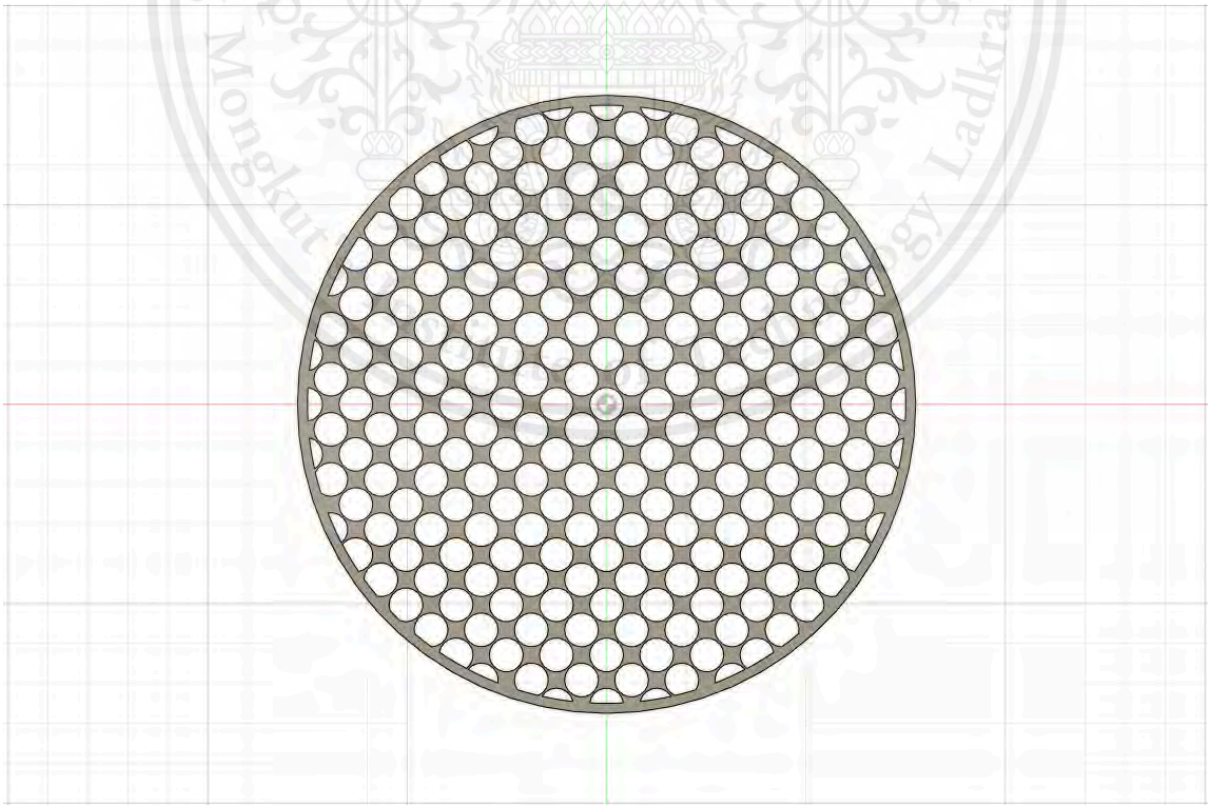

(Figure) 4.3.1 Top view perspective of circular honeycomb

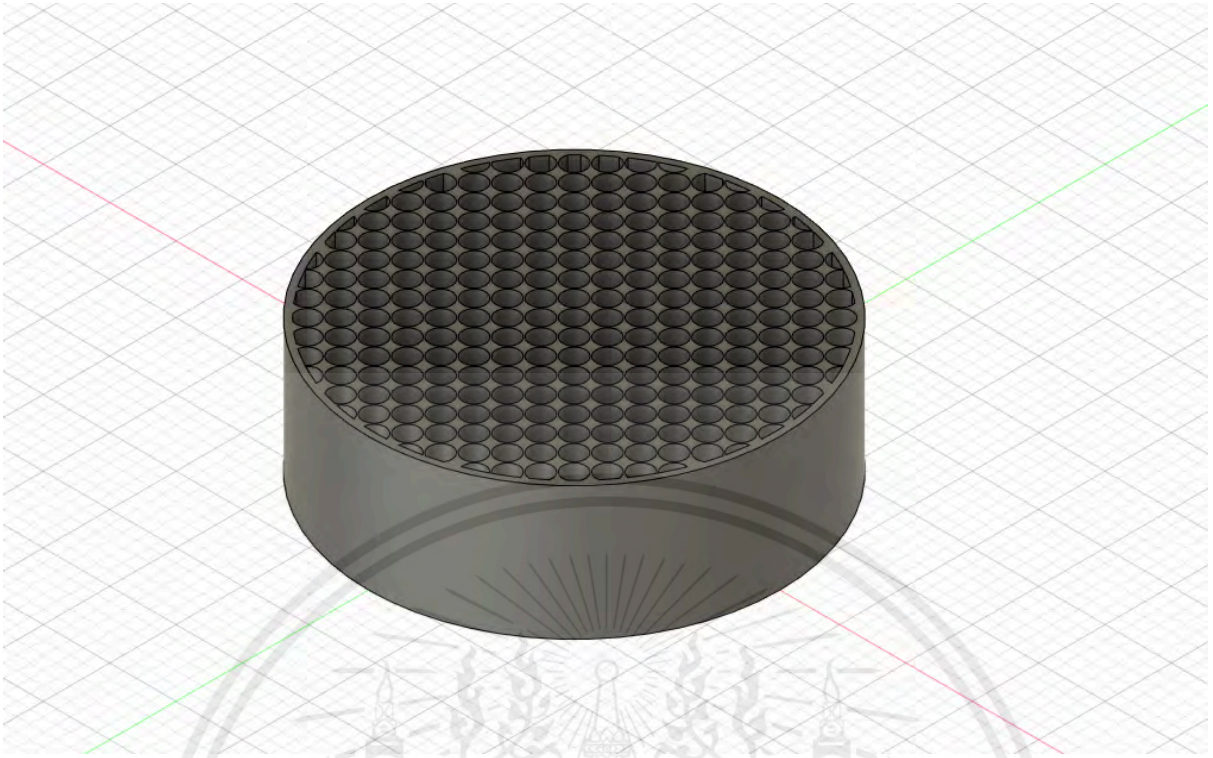

(Figure) 4.3.1.1 3D Circular honeycomb model

4.3.2 Square honeycomb

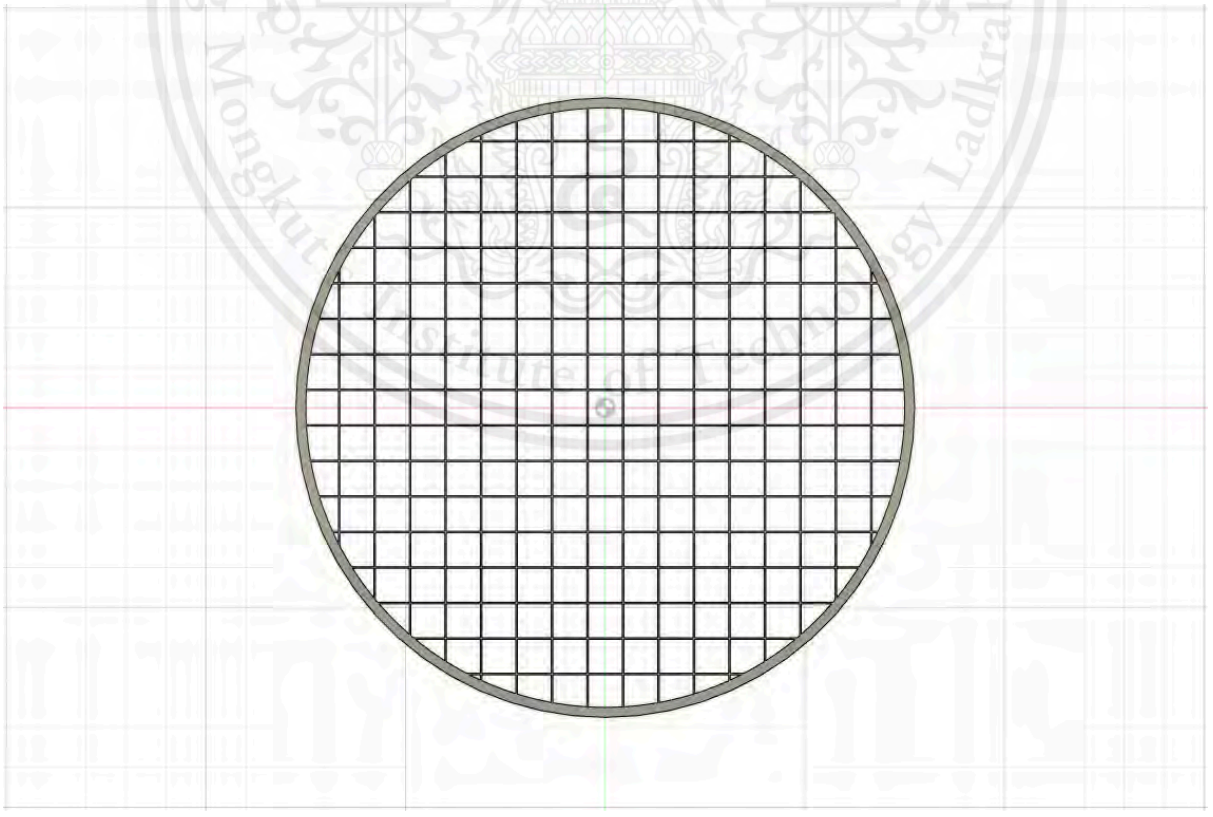

(Figure) 4.3.2 Top view perspective of square honeycomb

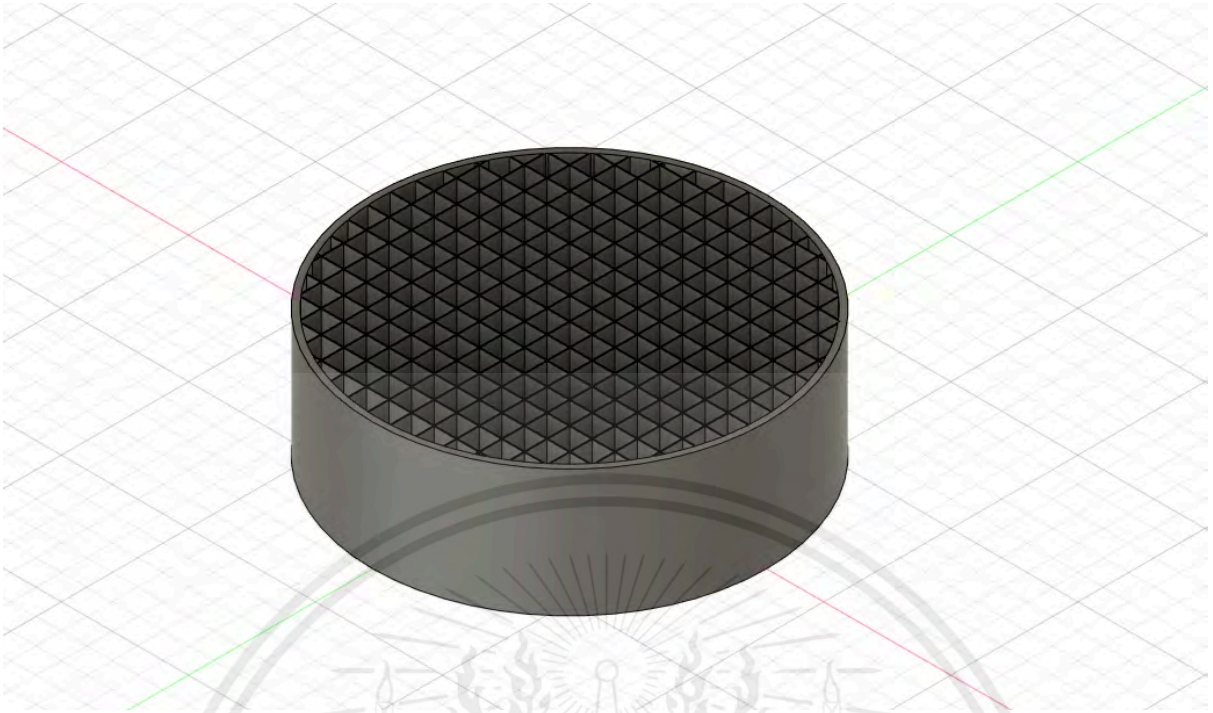

(Figure) 4.3.2.1 3D Square honeycomb model

4.2.3 Hexagonal Honeycomb

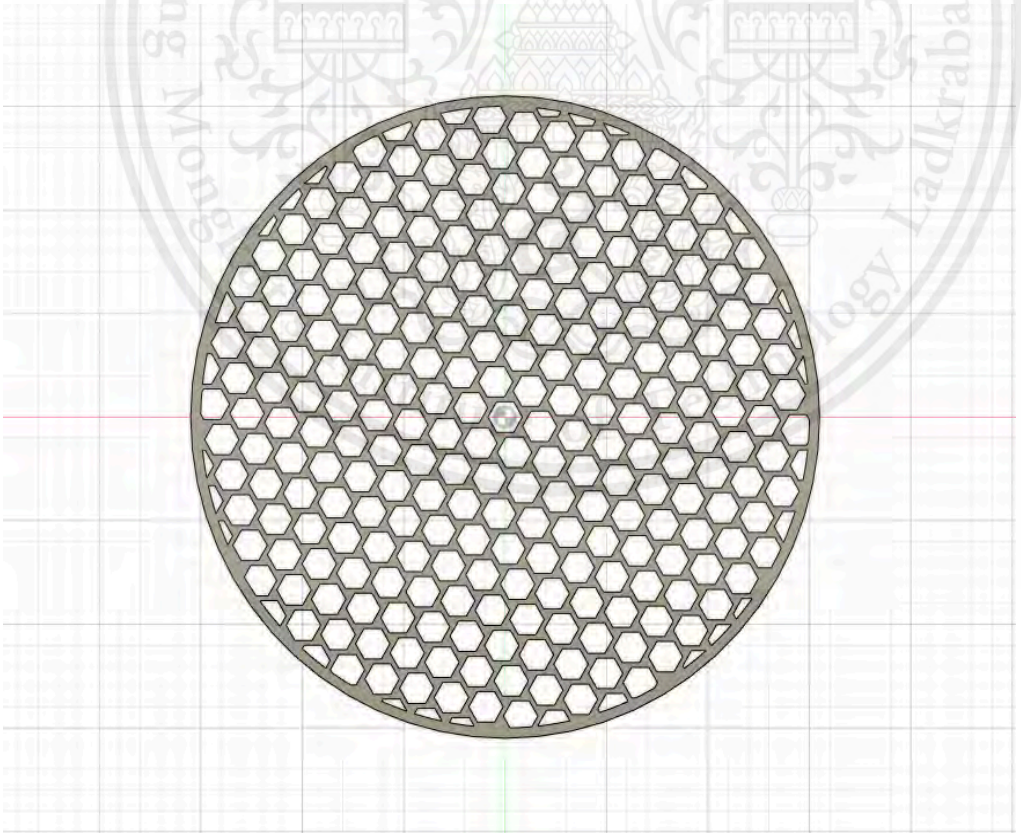

(Figure) 4.3.3 Top view perspective of hexagonal honeycomb

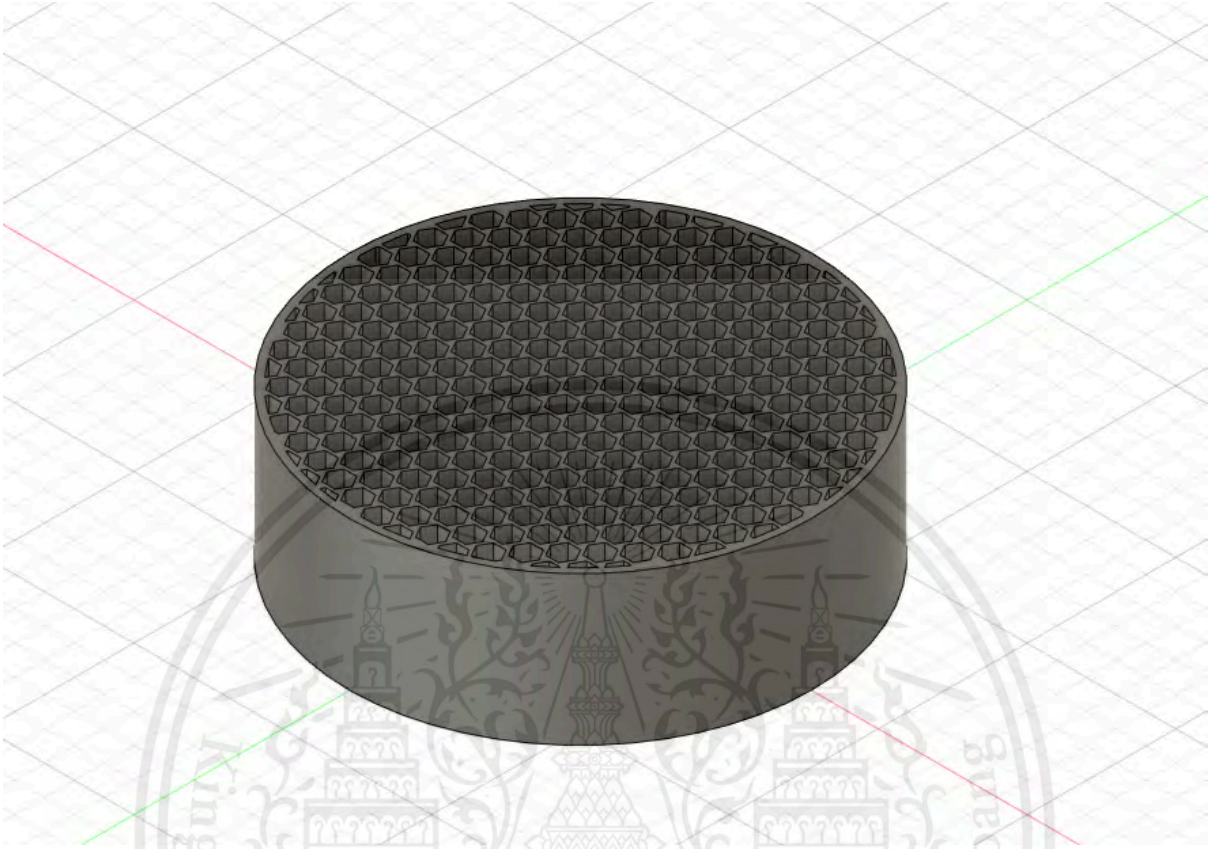

(Figure) 4.3.3.1 3D Hexagonal honeycomb model

4.2.4 Octagonal honeycomb

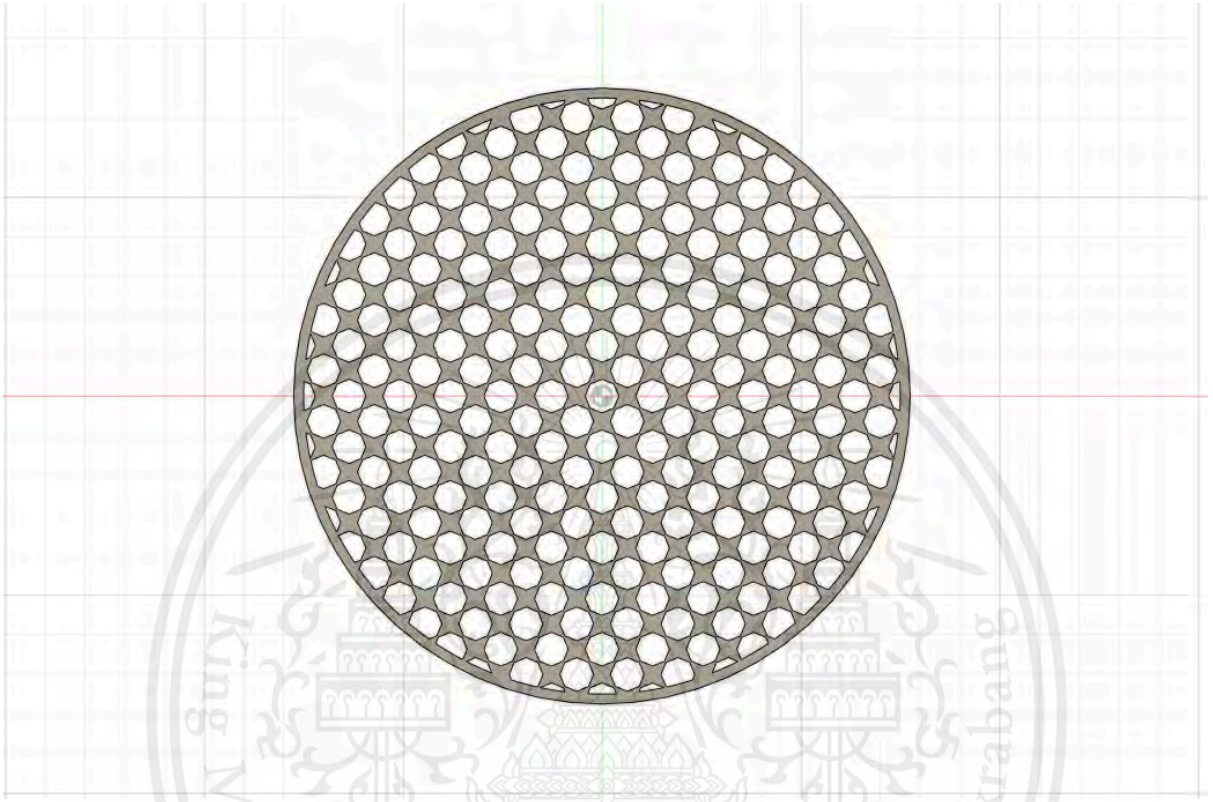

(Figure) 4.3.4 Top view perspective of octagonal honeycomb

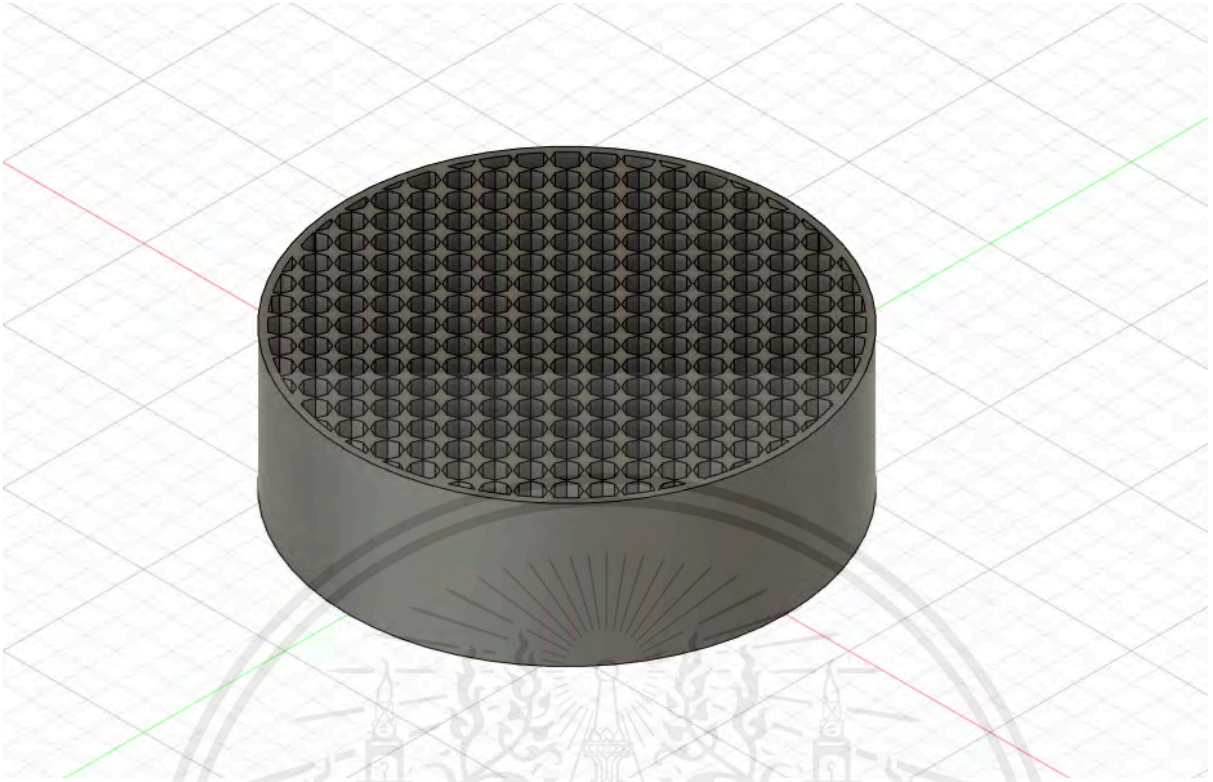

(Figure) 4.3.4 3D Octagonal honeycomb model

The process of designing these four models is almost identical to the process of designing models in Trial 1. The difference is the size of the grid which is 2.35 times smaller. The diameter or longest diagonal is reduced from 2 cm. to 0.85 cm.

Designs of both experiments are similar. However, the amount of grid in the honeycomb is different. On Trial 2, there is a greater amount of grid in each honeycomb to inspect if the size of the hole or grid would affect the result of the experiment which is turbulence intensity reduction in each design.

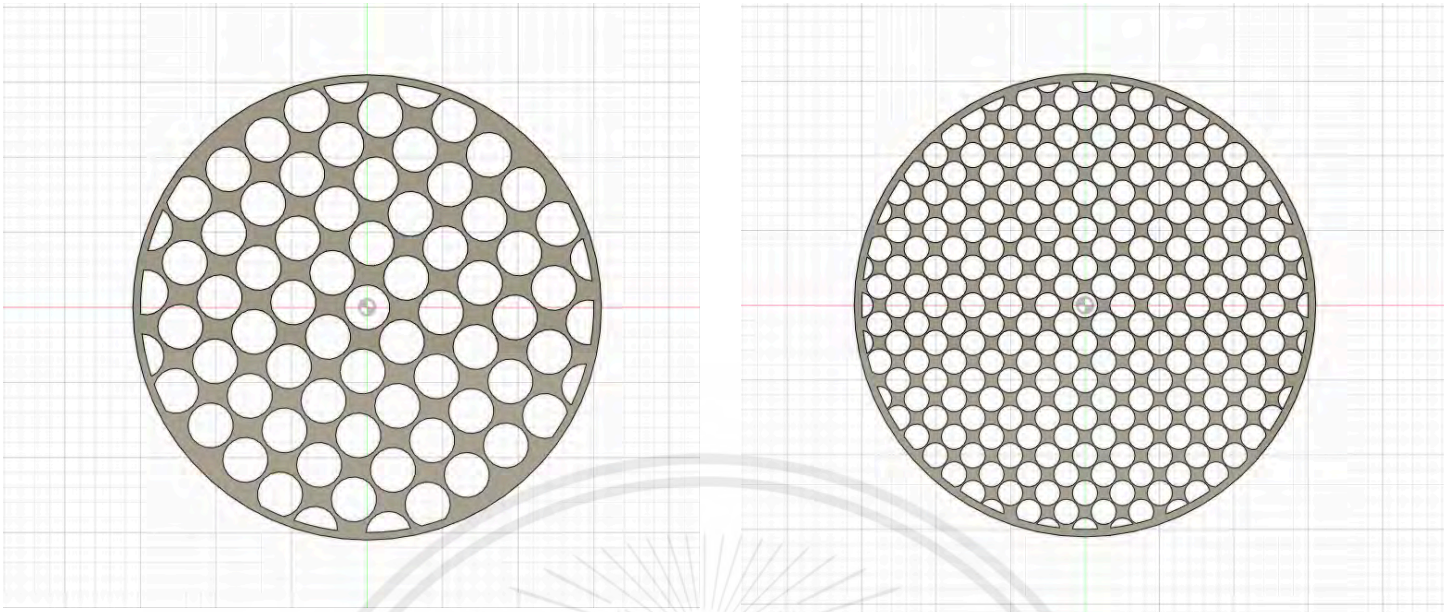

(Figure) 4.3.5 Trial 1 and Trial 2 grid size comparison of circular honeycomb

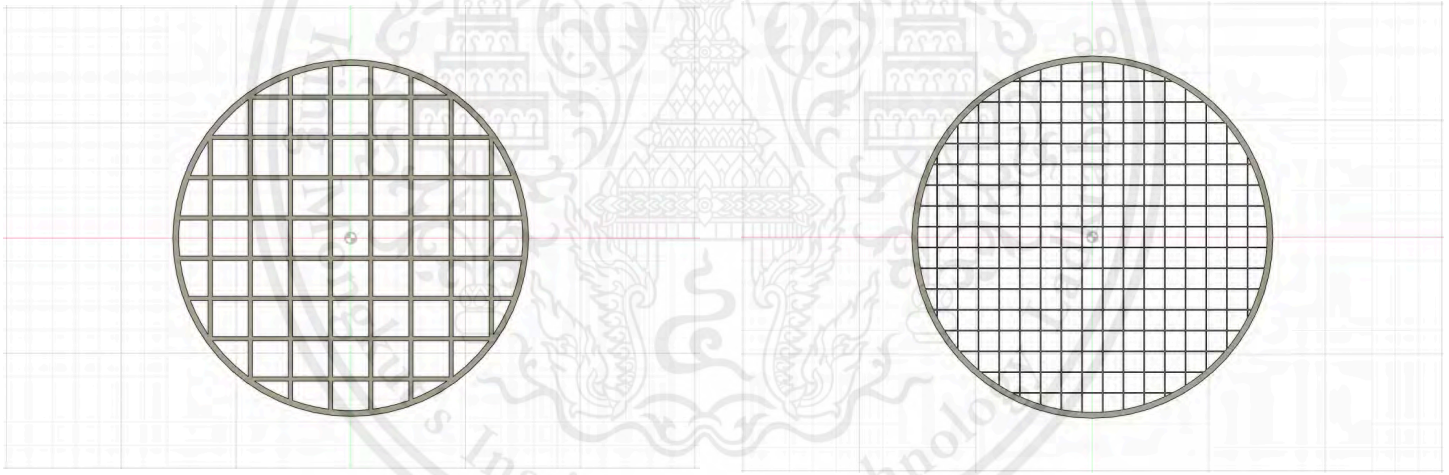

(Figure) 4.3.6 Trial 1 and Trial 2 grid size comparison of square honeycomb

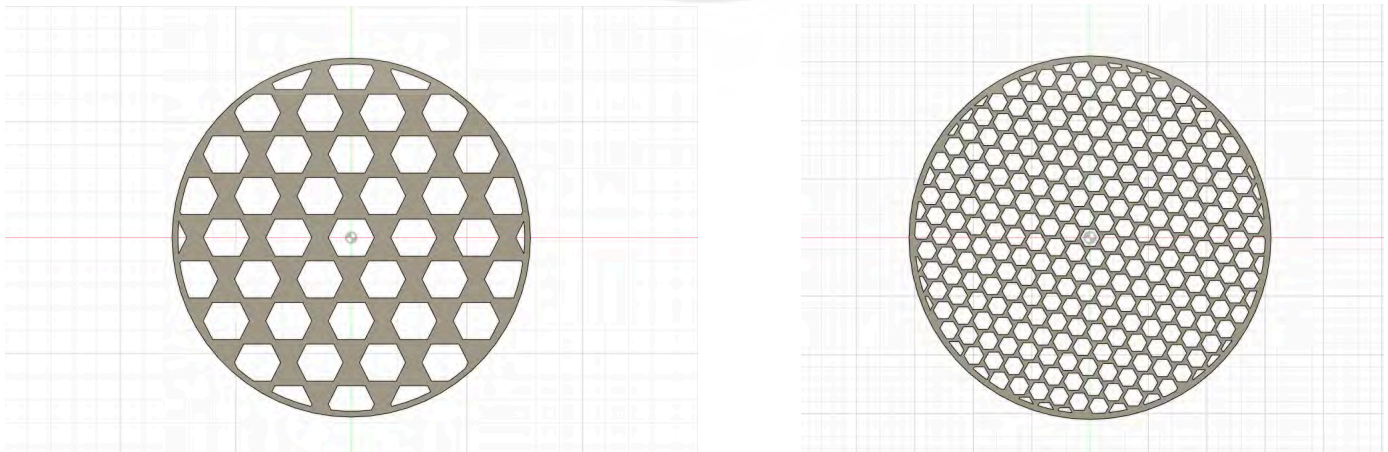

(Figure) 4.3.7 Trial 1 and Trial 2 grid size comparison of hexagonal honeycomb

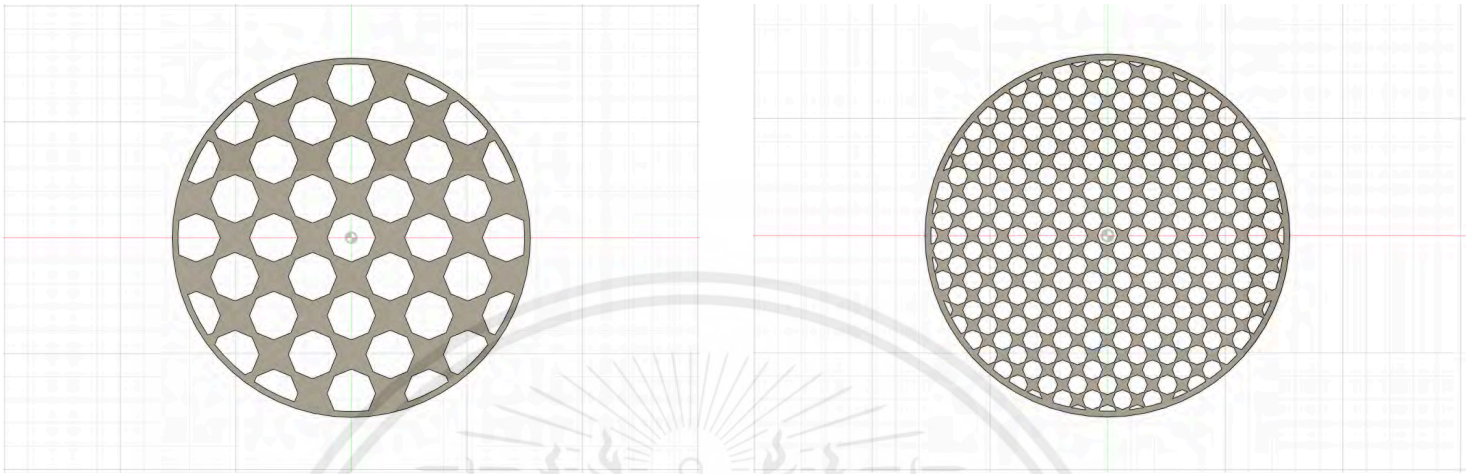

(Figure) 4.3.7 Trial 1 and Trial 2 grid size comparison of octagonal honeycomb

4.4 Simulation and Results

There are 4 shapes of honeycomb structure in our experiment. Each shape has 2 designs as mentioned in **4.3**. The reason is, there are limited resources for 3D printers. First design was too complicated in detail. The 3D printer is unable to print. Which has a 0.85 cm diameter of each cell. So, we have to change to a bigger mesh design which is 2.0 cm of cells. Thus, there are 8 simulations, including the first four designs and 4 actual designs that we print the 3D workpiece to test in the Wind tunnel workshop.

Through comprehensive testing within our simulation project, we have identified a crucial aspect regarding the design structure that needs to effectively address all gaps which wind may pass through, to ensure the most accuracy of the simulation. As a result, we have implemented a solution involving the creation of a virtual tube, which references the wind tunnel but is smaller in scale compared to the honeycomb structure. This strategic adjustment ensures that the boundaries of the honeycomb workpiece do not interfere with the internal flow dynamics of the simulation, thereby optimizing its accuracy and reliability..

All simulations are the same boundary conditions :

Inlet velocity: Normal to face is 10 m/s (Swirl).

Angular velocity: 330.2 rad/s (Assuming a normal wind tunnel with 10 m/s velocity of air).

Environment pressure: 101.325 kPa

Temperature: 293.2 K

4.4.1) 0.85 cm square honeycomb structure.

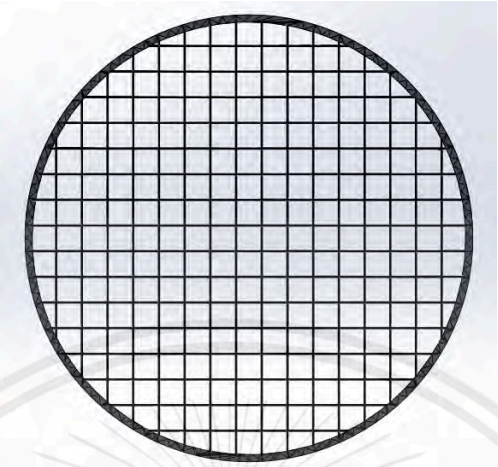

Figure 4.4.1.1

The initial phase of our project involved simulating the design by visualizing the wind tunnel for fluid flow analysis. This is for establishing boundary conditions, which included an inlet velocity of 10 m/s for the air. Additionally, we set the angular velocity of the twirling air to 330.2 rad/s as part of the simulation setup. These meticulously defined parameters served as the foundation for our subsequent analyses and evaluations within the project.

Subsequently, our primary analysis focused on generating a cross-sectional plot at the center of the honeycomb structure (Figure 4.4.1.2). This enabled us to visualize and comprehend the alterations in velocity subsequent to the passage of air through the workpiece.

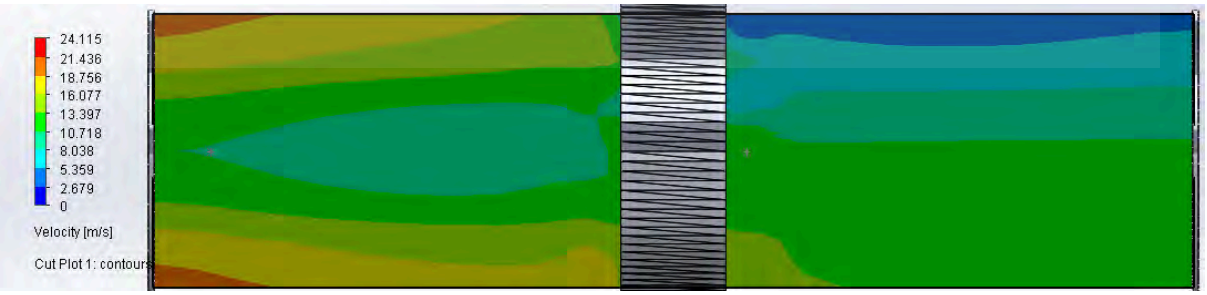

Figure 4.4.1.2 Velocity distribution

Next, we proceeded to insert a point goal to precisely measure the specific volume within the simulated environment. Our focus centered on key parameters within our setup, notably the velocity of the air both before and after traversing the honeycomb structure, as well as the turbulence intensity.

Summary

Goal Name	Unit	Value	Averaged Value	Minimum Value	Maximum Value	Progress [%]	Use In Convergence	Delta	Criteria
PG Static Pressure 1	[Pa]	101383.34	101383.22	101383.06	101383.36	100	Yes	0.30	167.82
PG Total Pressure 2	[Pa]	101451.56	101451.43	101451.26	101451.57	100	Yes	0.31	168.15
PG Dynamic Pressure 3	[Pa]	68.20	68.19	68.17	68.20	100	Yes	0.03	2.35
PG Velocity 4	[m/s]	10.620	10.619	10.617	10.620	100	Yes	0.003	0.200
PG Velocity (X) 5	[m/s]	-0.212	-0.213	-0.213	-0.212	100	Yes	2.118e-04	0.027
PG Velocity (Y) 6	[m/s]	-0.057	-0.057	-0.057	-0.057	100	Yes	1.871e-04	0.008
PG Velocity (Z) 7	[m/s]	-9.445	-9.444	-9.445	-9.443	100	Yes	0.002	0.330
PG Turbulence Length 8	[m]	0.002	0.002	0.002	0.002	100	Yes	3.061e-08	3.817e-05
PG Turbulence Intensity 9	[%]	2.20	2.20	2.20	2.20	100	Yes	4.54e-04	0.15
PG Turbulent Energy 10	[J/kg]	0.081	0.081	0.081	0.081	100	Yes	1.566e-05	0.007
PG Static Pressure 11	[Pa]	101321.69	101321.91	101321.62	101322.41	100	Yes	0.79	1.99
PG Total Pressure 12	[Pa]	101408.22	101408.48	101407.74	101409.32	100	Yes	1.58	8.78
PG Dynamic Pressure 13	[Pa]	86.50	86.55	85.96	86.97	100	Yes	1.01	8.62
PG Velocity 14	[m/s]	11.977	11.980	11.939	12.010	100	Yes	0.070	0.555
PG Velocity (X) 15	[m/s]	0.025	0.031	-0.003	0.066	100	Yes	0.034	0.037
PG Velocity (Y) 16	[m/s]	-0.129	-0.086	-0.159	-0.026	100	Yes	0.025	0.145
PG Velocity (Z) 17	[m/s]	-11.968	-11.972	-12.000	-11.933	100	Yes	0.067	0.559
PG Turbulence Length 18	[m]	0.001	0.001	0.001	0.001	100	Yes	1.823e-05	7.760e-05
PG Turbulence Intensity 19	[%]	3.54	3.57	3.52	3.61	100	Yes	0.09	0.44
PG Turbulent Energy 20	[J/kg]	0.272	0.276	0.270	0.283	100	Yes	0.013	0.051
Velocity Change	[m/s]	-1.358	-1.361	-1.390	-1.320	100	Yes	0.070	0.594

Inlet velocity	10.620	m/s
Outlet velocity	11.977	m/s
Turbulence intensity change	1.34	%
Average velocity change	Faster 1.361	m/s

To provide a clearer understanding of the turbulence distribution achieved by the honeycomb structure, we implemented Flow Trajectories(Figure 4.4.1.3) analysis. This method allowed us to observe and analyze the changes in wind flow patterns as it interacts with the structure.

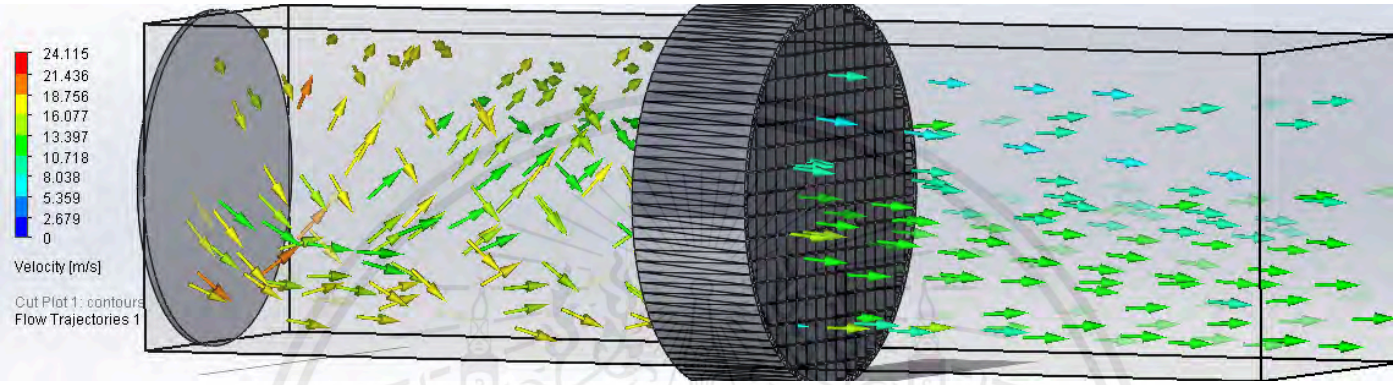

Figure 4.4.1.3 Flow Trajectory

By visualizing the trajectory of the flow, we gained valuable insights into how the honeycomb structure effectively mitigates turbulence, contributing to a smoother and more controlled airflow within the simulated environment.

From Figure 4.4.1.3, the 0.85 square-shaped honeycomb structure exhibits promising potential for reducing turbulence. When entering the honeycomb, the swirling air tends to transition towards a laminar flow pattern, as depicted in the analysis. Despite the observed fluctuations in velocity flow, as illustrated in Figure 4.4.1.2, the honeycomb filter notably contributes to turbulence distribution.

4.4.2) 2.0 cm square honeycomb structure.

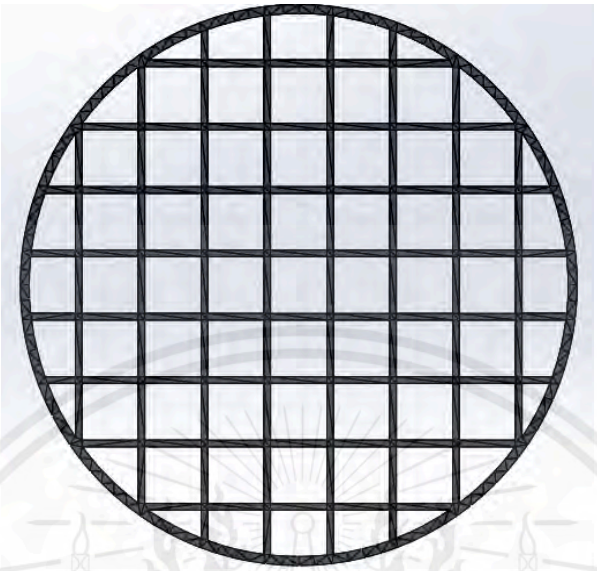

Figure 4.4.2.1

The comparison between Figure 4.4.2.1 and Figure 4.4.1.1 reveals notable differences in the mesh structure and size of the square cell. It is evident that the mesh and cell size in Figure 4.4.2.1 are considerably larger compared to those in Figure 4.4.1.1. This discrepancy raises concerns regarding the potential effectiveness of the design relative to the 0.85 cm square honeycomb.

Following a similar approach as the previous design iteration, we initiated the simulation process by setting up the necessary boundary conditions for the new design variation. Then use the cut plot tool for analyze the middle velocity flow.

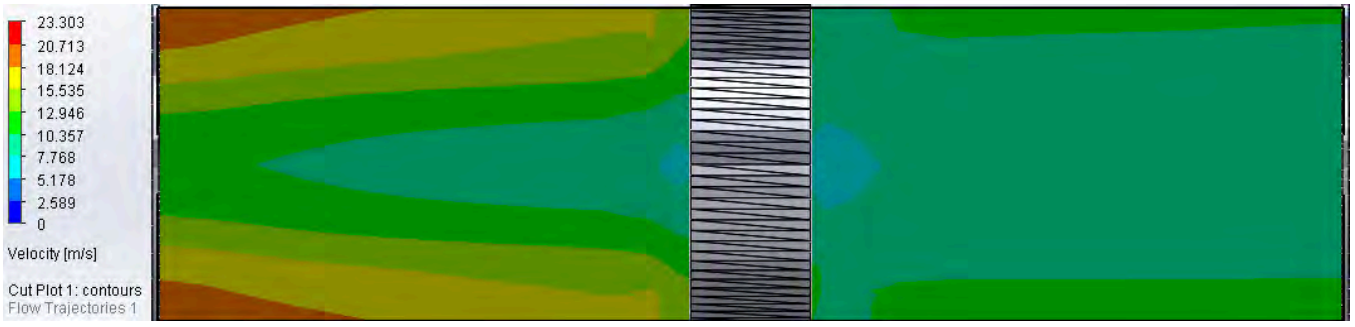

Figure 4.4.2.2 Velocity distribution

Ensure that the objective is set to attain the required value.

Summary

Goal Name	Unit	Value	Averaged Value	Minimum Value	Maximum Value	Progress [%]	Use In Convergence	Delta	Criteria
PG Static Pressure 1	[Pa]	101331.12	101331.90	101331.12	101333.69	100	Yes	2.58	73.60
PG Dynamic Pressure 2	[Pa]	68.15	68.10	68.00	68.15	100	Yes	0.15	2.32
PG Velocity 3	[m/s]	10.626	10.622	10.613	10.626	100	Yes	0.013	0.194
PG Velocity (X) 4	[m/s]	-0.027	-0.027	-0.027	-0.027	100	Yes	2.110e-04	0.005
PG Velocity (Y) 5	[m/s]	0.121	0.121	0.121	0.121	100	Yes	2.432e-04	0.015
PG Velocity (Z) 6	[m/s]	-9.478	-9.474	-9.478	-9.467	100	Yes	0.011	0.325
PG Turbulence Length 7	[m]	0.002	0.002	0.002	0.002	100	Yes	1.608e-07	3.818e-05
PG Turbulence Intensity 8	[%]	2.19	2.19	2.19	2.19	100	Yes	2.85e-03	0.14
PG Turbulent Energy 9	[J/kg]	0.081	0.081	0.081	0.081	100	Yes	7.484e-06	0.007
PG Static Pressure 10	[Pa]	101327.18	101327.43	101327.18	101327.85	100	Yes	0.67	1.25
PG Dynamic Pressure 11	[Pa]	42.49	42.79	42.45	44.52	100	Yes	2.07	7.44
PG Velocity 12	[m/s]	8.402	8.432	8.398	8.600	100	Yes	0.202	0.594
PG Velocity (X) 13	[m/s]	0.030	0.027	-0.005	0.053	100	Yes	0.012	0.019
PG Velocity (Y) 14	[m/s]	-0.053	-0.041	-0.055	-0.019	100	Yes	0.013	0.019
PG Velocity (Z) 15	[m/s]	-8.401	-8.430	-8.599	-8.397	100	Yes	0.202	0.594
PG Turbulence Length 16	[m]	0.002	0.002	0.002	0.002	100	Yes	1.090e-04	1.218e-04
PG Turbulence Intensity 17	[%]	2.85	2.83	2.72	2.86	100	Yes	0.14	0.28
PG Turbulent Energy 18	[J/kg]	0.086	0.086	0.082	0.087	100	Yes	0.005	0.010
Velocity Change	[m/s]	2.224	2.191	2.014	2.225	100	Yes	0.211	0.755

Inlet velocity	10.626	m/s
Outlet velocity	8.432	m/s
Turbulence intensity change	0.66	%
Average velocity change	Slower 2.224	m/s

The primary distinction between the two designs lies in the frequency and size of cells within the honeycomb structure. It becomes apparent that the 2.0cm honeycomb variant

disperses airflow but it's slowing down the velocity of air which can be affected the ability of turbulence distribution.

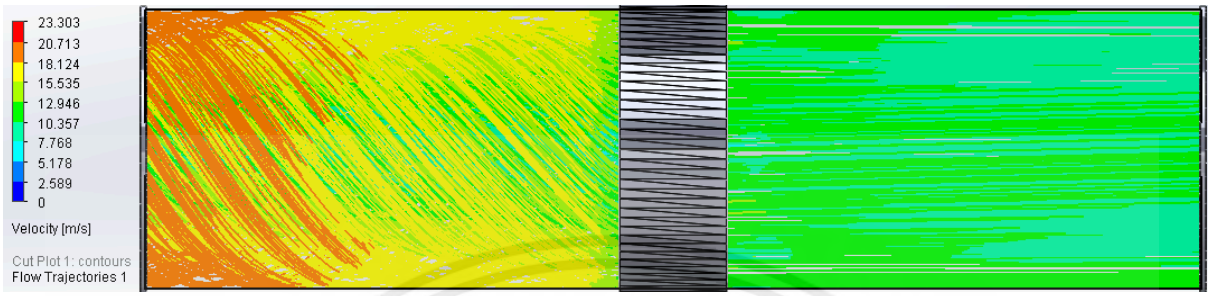

Figure 4.4.2.3 Velocity trajectories flow

After input the flow trajectory to the design. Apparently that the turbulence of this design has been distributed more. The reason is by slowing down the airflow, this design variation demonstrates potential for enhancing turbulence reduction within the simulated environment.

Turbulence intensity is a measure of the degree of fluctuation or irregularity in the flow field. When airflow is slowed down, it reduces the kinetic energy and velocity gradients within the flow, which in turn tends to decrease turbulence intensity.

4.4.3) 0.85 cm circular honeycomb structure.

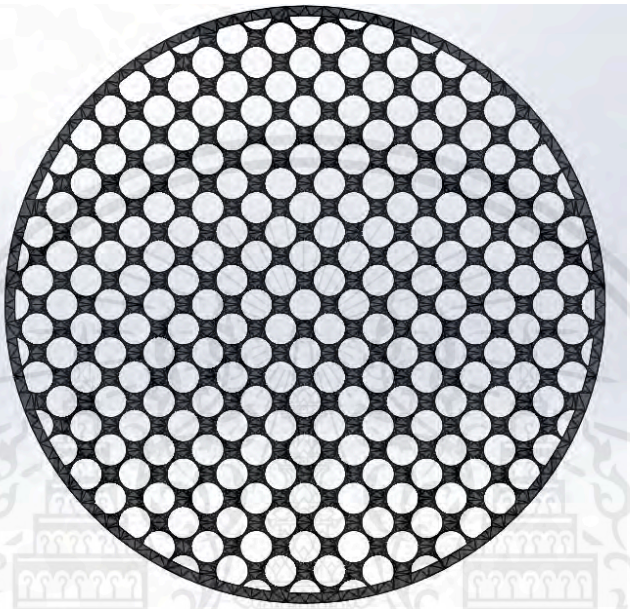

Figure 4.4.3.1

Among the various honeycomb designs, the circular honeycomb stands apart as the sole structure lacking edges. This unique characteristic offers a distinctive opportunity to explore the impact of cell edges on both air velocity and turbulence levels. By comparing the circular honeycomb with other designs featuring edges, we can gain insights into how the presence or absence of edges influences airflow dynamics and turbulence within the structure. This analysis provides valuable information for optimizing honeycomb designs to achieve desired airflow characteristics and turbulence reduction in various engineering applications.

Figure 4.4.3.2 Velocity distribution

Goal Name	Unit	Value	Averaged Value	Minimum Value	Maximum Value	Progress [%]	Use In Convergence	Delta	Criteria
PG Static Pressure 1	[Pa]	106339.95	106375.95	106339.95	106421.13	100	Yes	81.18	8649.94
PG Total Pressure 2	[Pa]	106413.91	106450.05	106413.91	106495.39	100	Yes	81.47	8645.59
PG Dynamic Pressure 3	[Pa]	73.95	74.08	73.95	74.24	100	Yes	0.29	4.38
PG Velocity 4	[m/s]	10.805	10.812	10.805	10.822	100	Yes	0.017	0.655
PG Velocity (X) 5	[m/s]	0.002	0.002	0.002	0.002	100	Yes	3.224e-05	0.001
PG Velocity (Y) 6	[m/s]	-0.062	-0.062	-0.062	-0.062	100	Yes	3.671e-05	0.009
PG Velocity (Z) 7	[m/s]	-9.334	-9.343	-9.353	-9.334	100	Yes	0.019	0.483
PG Turbulence Length 8	[m]	0.002	0.002	0.002	0.002	100	Yes	8.963e-08	3.416e-05
PG Turbulence Intensity 9	[%]	2.25	2.24	2.24	2.25	100	Yes	3.69e-03	0.05
PG Turbulent Energy 10	[J/kg]	0.088	0.088	0.088	0.088	100	Yes	3.300e-06	0.007
PG Static Pressure 11	[Pa]	101273.92	101276.66	101273.92	101279.46	100	Yes	1.84	34.43
PG Total Pressure 12	[Pa]	101335.50	101338.15	101335.46	101341.68	100	Yes	1.38	37.65
PG Dynamic Pressure 13	[Pa]	61.55	61.47	60.35	63.27	100	Yes	1.00	4.70
PG Velocity 14	[m/s]	9.447	9.371	9.243	9.559	100	Yes	0.045	0.554
PG Velocity (X) 15	[m/s]	-0.165	-0.222	-0.302	-0.163	100	Yes	0.075	0.100
PG Velocity (Y) 16	[m/s]	0.073	0.344	0.073	0.609	100	Yes	0.122	0.135
PG Velocity (Z) 17	[m/s]	-9.219	-9.107	-9.304	-8.958	100	Yes	0.023	0.576
PG Turbulence Length 18	[m]	9.364e-04	9.209e-04	9.037e-04	9.393e-04	100	Yes	3.559e-05	1.832e-04
PG Turbulence Intensity 19	[%]	7.94	8.14	7.85	8.34	100	Yes	0.20	0.70
PG Turbulent Energy 20	[J/kg]	0.689	0.694	0.680	0.712	100	Yes	0.032	0.066
Velocity change	[m/s]	1.358	1.442	1.246	1.574	100	Yes	0.029	1.048

Inlet velocity	10.8805	m/s
Outlet velocity	9.447	m/s
Turbulence intensity change	Increase 5.69	%
Average velocity change	Slower 1.358	m/s

The velocity of this design exhibits minimal variation, as shown in Figure 4.4.3.2. However, it is notable that airflow encounters resistance when entry into the honeycomb structure, resulting poorly in a reduction of turbulence within the system. The turbulence intensity has exhibited considerable variability. There is no smooth flow profile as shown in Figure 4.4.3.3.

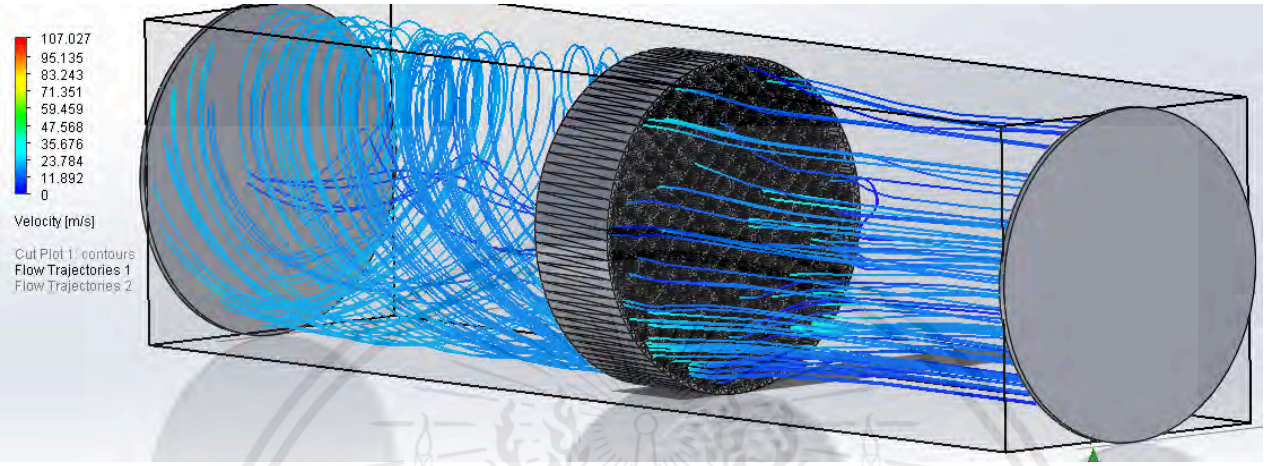

Figure 4.4.3.3 Flow trajectory

The flow trajectory analysis indicates that the swirling air flow passing through the model results in a suboptimal laminar flow upon exiting. Significant turbulence persists even after the airflow has traversed the filter with the faster air velocity.

Based on Figure 4.4.3.3, it is evident that achieving a smooth airflow is unattainable with this design. Circular honeycomb structures are not commonly utilized due to challenges in production and structural weaknesses compared to other shapes. Additionally, their flow capabilities do not surpass all other alternative designs.

4.4.4) 2.0 cm circular honeycomb structure.

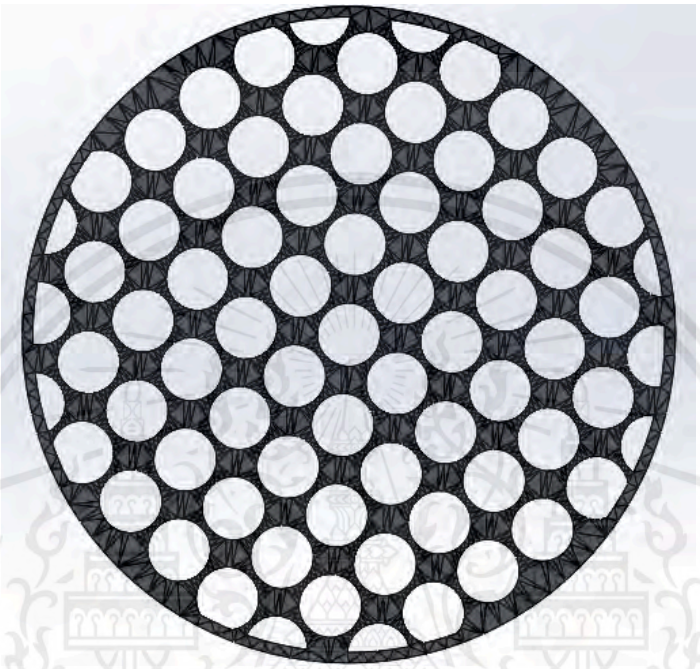

Figure 4.4.4.1

Compared to the 2.0 octagon and 2.0 hexagon designs, the 2.0 circular shape exhibits the smallest gap within each cell. Its format and structure closely resemble those of the 0.85 design, except for the cell size.

The circular design boasts the highest level of detail in its 3D representation. This is attributed to its large solid file size, which results in longer simulation times, particularly evident in the case of the 0.85 cm circular honeycomb.

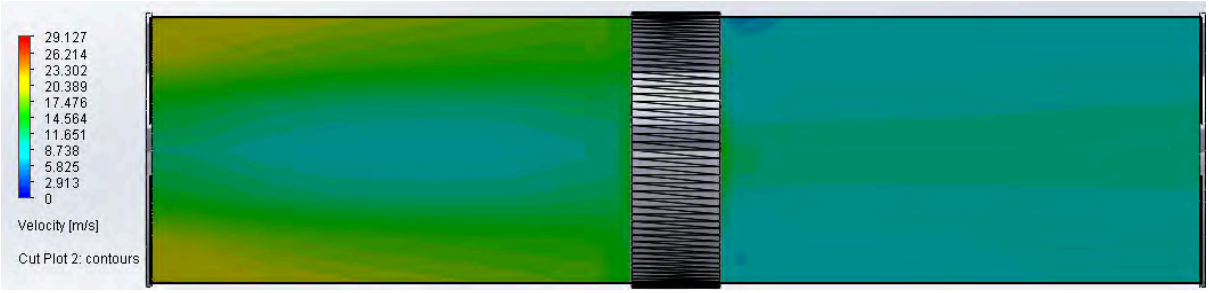

Figure 4.4.4.2 Velocity distribution

Evidence from Figure 4.4.4.2, when compared to Figure 4.4.3.2, demonstrates that the 0.85 circular honeycomb design exhibits superior velocity distribution characteristics. Unlike the 2.0 circular honeycomb, which doesn't decelerate velocity uniformly, it instead results in velocity increased on certain surfaces of the structure.

Goal Name	Unit	Value	Averaged Value	Minimum Value	Maximum Value	Progress [%]	Use In Convergence	Delta	Criteria
PG Static Pressure 1	[Pa]	101666.69	101667.08	101666.66	101667.92	100	Yes	1.26	150.37
PG Total Pressure 2	[Pa]	101722.74	101722.91	101722.57	101723.42	100	Yes	0.85	153.02
PG Dynamic Pressure 3	[Pa]	56.03	55.81	55.49	56.03	100	Yes	0.55	5.99
PG Velocity 4	[m/s]	9.588	9.568	9.539	9.588	100	Yes	0.049	0.555
PG Velocity (X) 5	[m/s]	-0.183	-0.183	-0.183	-0.182	100	Yes	8.989e-04	0.025
PG Velocity (Y) 6	[m/s]	0.112	0.111	0.111	0.112	100	Yes	5.283e-04	0.015
PG Velocity (Z) 7	[m/s]	-8.241	-8.224	-8.241	-8.198	100	Yes	0.043	0.716
PG Turbulence Length 8	[m]	0.002	0.002	0.002	0.002	100	Yes	6.693e-07	4.482e-05
PG Turbulence Intensity 9	[%]	2.62	2.62	2.62	2.63	100	Yes	0.01	0.30
PG Turbulent Energy 10	[J/kg]	0.094	0.093	0.093	0.094	100	Yes	1.155e-04	0.010
PG Static Pressure 11	[Pa]	101305.80	101306.06	101305.72	101306.65	100	Yes	0.93	6.97
PG Total Pressure 12	[Pa]	101382.01	101382.41	101381.71	101382.94	100	Yes	1.23	11.12
PG Dynamic Pressure 13	[Pa]	76.19	76.33	75.90	76.82	100	Yes	0.92	5.96
PG Velocity 14	[m/s]	11.245	11.255	11.223	11.292	100	Yes	0.069	0.416
PG Velocity (X) 15	[m/s]	0.008	0.056	0.008	0.126	100	Yes	0.032	0.034
PG Velocity (Y) 16	[m/s]	0.098	0.087	0.031	0.135	100	Yes	0.031	0.097
PG Velocity (Z) 17	[m/s]	-11.233	-11.242	-11.278	-11.211	100	Yes	0.067	0.419
PG Turbulence Length 18	[m]	0.002	0.002	0.002	0.002	100	Yes	1.145e-05	1.055e-04
PG Turbulence Intensity 19	[%]	2.69	2.70	2.68	2.73	100	Yes	0.05	0.37
PG Turbulent Energy 20	[J/kg]	0.145	0.147	0.145	0.149	100	Yes	0.004	0.051
Velo Change	[m/s]	-1.658	-1.687	-1.716	-1.652	100	Yes	0.064	0.937

Inlet velocity	9.588	m/s
Outlet velocity	11.245	m/s
Turbulence intensity change	0.07	%
Average velocity change	Faster 1.658	m/s

Even the average velocity of the 2.0 circular honeycomb is increasing but in terms of turbulence intensity is surprisingly good.

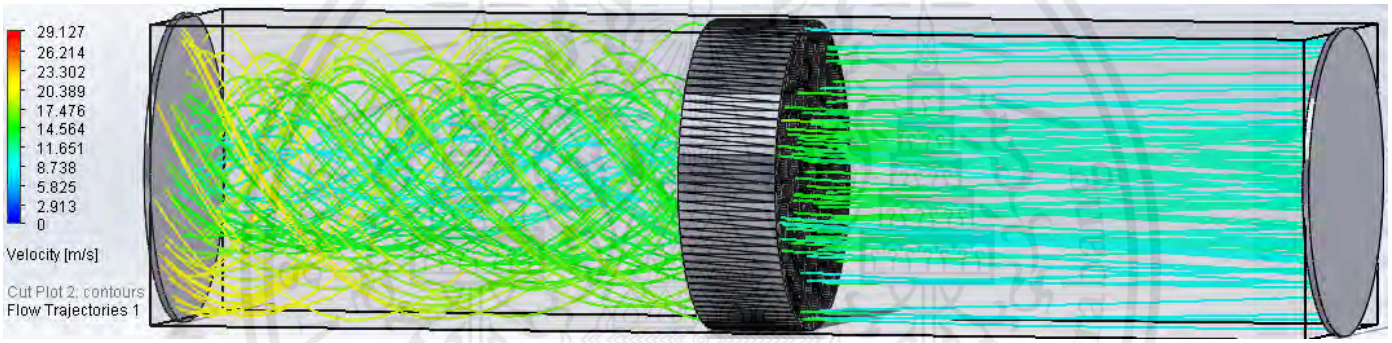

Figure 4.4.4.3 Velocity Flow trajectory

Figure 4.4.4.3 illustrates a notable transition from turbulent to laminar flow, which is more effectively achieved compared to the 0.85 circular honeycomb design. This improvement is attributed to the larger circular cell size. However, a significant issue arises with this design, as the airflow velocity fluctuates considerably and lacks uniformity.

4.4.5) 0.85 cm Hexagon honeycomb structure.

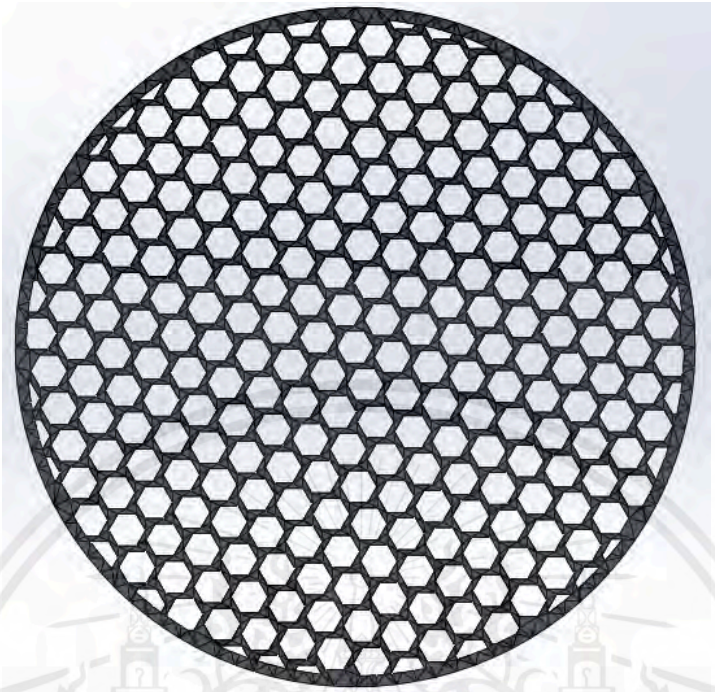

Figure 4.4.5.1

The hexagon honeycomb structure stands as the commonly used in aircraft and other aerodynamically critical industries due to its exceptional strength and superior performance across various capabilities, placing it at the forefront of industry standards.

Hexagons provide the most efficient use of space, allowing for maximum strength and stability with minimal material usage. Additionally, hexagons have equal edge lengths and angles, resulting in a uniform and symmetrical structure. This uniformity helps distribute loads

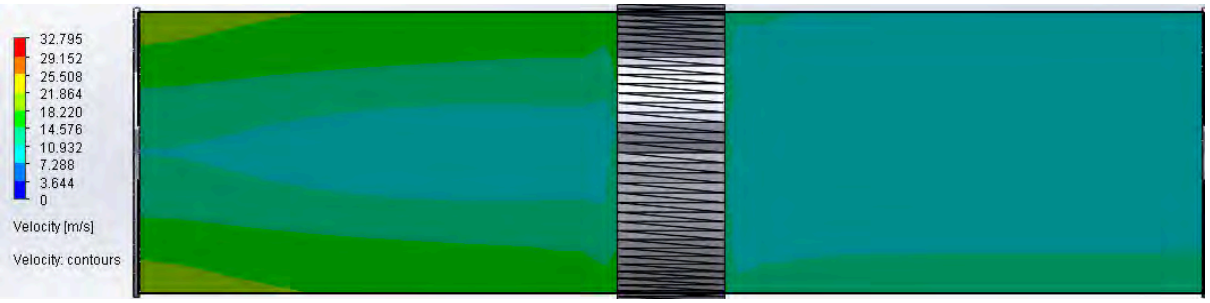

Figure 4.4.5.1 Velocity distribution

The hexagonal shape promotes smoother airflow compared to other shapes, reducing aerodynamic drag and improving overall efficiency. Figure 4.4.5.1 obviously shows that the turbulence flow changes to laminar flow with constant velocity orderly.

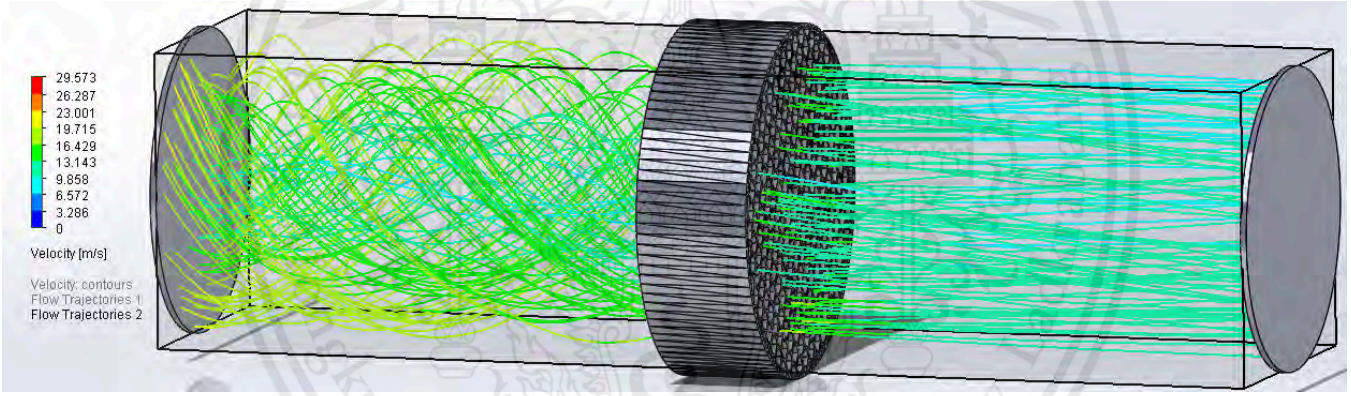

Figure 4.4.5.2 Flow trajectory

The flow trajectory of the 0.85 hexagon honeycomb demonstrates excellent characteristics, with airflow remaining highly laminar post-filter. The inherent structure and edges of the hexagon shape contribute positively to airflow, resulting in consistent velocity distribution without significant fluctuations.

Goal Name	Unit	Value	Averaged Value	Minimum Value	Maximum Value	Progress [%]	Use In Convergence	Delta	Criteria
PG Static Pressure 1	[Pa]	101288.96	101288.79	101288.08	101289.33	100	Yes	1.25	9.88
PG Total Pressure 2	[Pa]	101345.29	101345.04	101343.27	101347.23	100	Yes	1.23	9.85
PG Dynamic Pressure 3	[Pa]	56.31	56.23	54.69	57.88	100	Yes	3.19	4.37
PG Velocity 4	[m/s]	8.903	8.903	8.797	9.047	100	Yes	0.095	0.226
PG Velocity (X) 5	[m/s]	0.208	0.107	-0.032	0.288	100	Yes	0.038	0.053
PG Velocity (Y) 6	[m/s]	0.353	0.244	0.113	0.355	100	Yes	0.023	0.040
PG Velocity (Z) 7	[m/s]	-8.866	-8.871	-9.005	-8.771	100	Yes	0.092	0.224
PG Turbulence Length 8	[m]	0.002	0.002	0.002	0.002	100	Yes	1.283e-04	1.589e-04
PG Turbulence Intensity 9	[%]	14.46	14.69	14.19	15.46	100	Yes	1.27	2.64
PG Turbulent Energy 10	[J/kg]	1.624	1.662	1.581	1.842	100	Yes	0.260	0.330
PG Static Pressure 11	[Pa]	101880.67	101883.06	101880.67	101888.96	100	Yes	8.29	506.50
PG Total Pressure 12	[Pa]	101949.77	101952.12	101949.77	101957.94	100	Yes	8.17	508.02
PG Dynamic Pressure 13	[Pa]	69.08	69.05	68.96	69.08	100	Yes	0.12	2.26
PG Velocity 14	[m/s]	10.654	10.651	10.643	10.654	100	Yes	0.010	0.192
PG Velocity (X) 15	[m/s]	0.324	0.324	0.324	0.324	100	Yes	4.807e-04	0.039
PG Velocity (Y) 16	[m/s]	0.125	0.125	0.125	0.125	100	Yes	1.585e-04	0.018
PG Velocity (Z) 17	[m/s]	-9.445	-9.443	-9.445	-9.436	100	Yes	0.008	0.311
PG Turbulence Length 18	[m]	0.015	0.015	0.015	0.015	100	Yes	9.044e-09	3.150e-04
PG Turbulence Intensity 19	[%]	7.54	7.55	7.54	7.55	100	Yes	9.43e-03	0.75
PG Turbulent Energy 20	[J/kg]	0.961	0.961	0.961	0.961	100	Yes	3.863e-04	0.116
Velocity Change	[m/s]	-1.750	-1.747	-1.854	-1.602	100	Yes	0.134	0.396

Inlet velocity	8.903	m/s
Outlet velocity	10.654	m/s
Turbulence intensity change	Decrease 4.33	%
Average velocity change	Increase 1.750	m/s

The velocity of the airflow remains relatively constant, indicating stability. Additionally, the favorable trends observed in airflow and turbulence intensity suggest a predominantly stable and laminar flow. Therefore, the flow can be characterized as stable and featuring a primarily laminar flow pattern.

4.4.6) 2.0 cm Hexagon honeycomb structure.

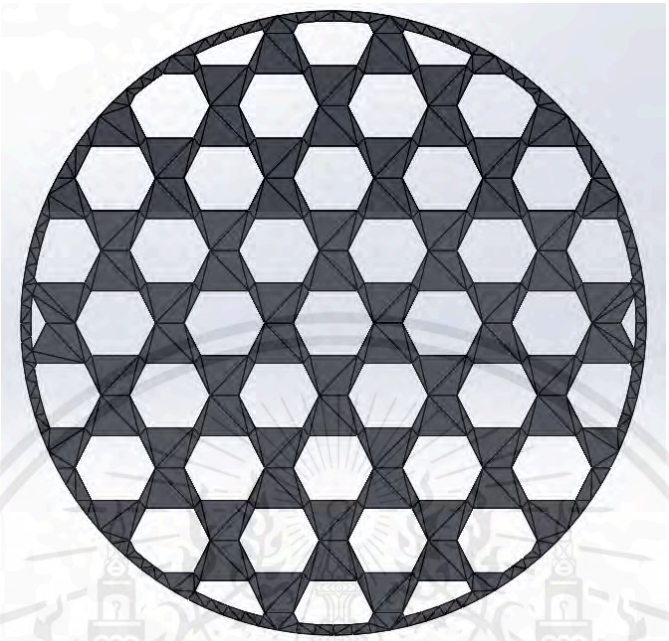

Figure 4.4.6.1

This 3D design is not the same as the one presented in section 4.4.5, exhibiting variations in both cell pattern and size. The size of each cell's gap needs to be increased to accommodate printing capabilities on a 3D printer. There is a possibility that the solid piece may obstruct the airflow.

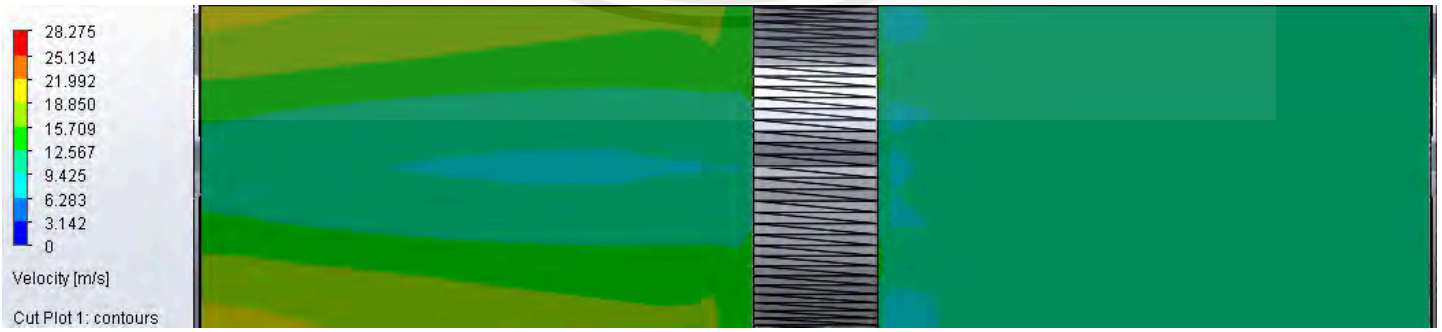

Figure 4.4.6.2 Velocity distribution

From Figure 4.4.6.2, it is evident that the airflow is hindered due to the presence of large solid gaps, resulting in minimal change in air velocity. However, despite this obstruction, the airflow manages to transition into a laminar flow pattern.

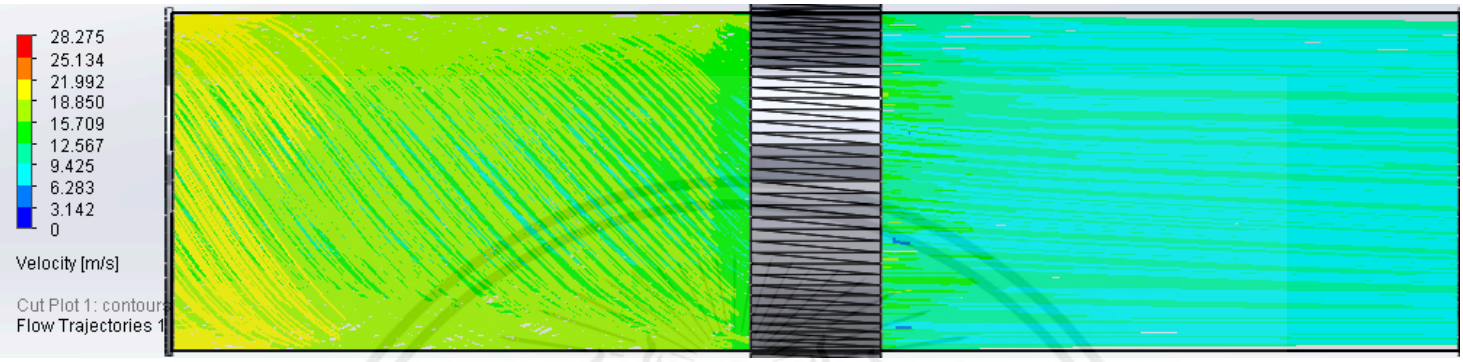

Figure 4.4.6.3 Flow trajectory

Summary

Goal Name	Unit	Value	Averaged Value	Minimum Value	Maximum Value	Progress [%]	Use In Convergence	Delta	Criteria
PG Static Pressure 1	[Pa]	101684.20	101684.62	101683.66	101688.05	100	Yes	4.39	92.37
PG Total Pressure 2	[Pa]	101754.88	101755.27	101754.33	101758.63	100	Yes	4.30	92.22
PG Dynamic Pressure 3	[Pa]	70.66	70.64	70.56	70.66	100	Yes	0.10	1.63
PG Velocity 4	[m/s]	10.804	10.801	10.795	10.804	100	Yes	0.008	0.136
PG Velocity (X) 5	[m/s]	-0.035	-0.035	-0.035	-0.034	100	Yes	1.745e-04	0.005
PG Velocity (Y) 6	[m/s]	-0.127	-0.127	-0.127	-0.127	100	Yes	8.257e-05	0.011
PG Velocity (Z) 7	[m/s]	-9.624	-9.622	-9.624	-9.617	100	Yes	0.007	0.254
PG Turbulence Length 8	[m]	0.002	0.002	0.002	0.002	100	Yes	1.548e-07	3.959e-05
PG Turbulence Intensity 9	[%]	2.14	2.14	2.14	2.14	100	Yes	1.75e-03	0.11
PG Turbulent Energy 10	[J/kg]	0.080	0.080	0.080	0.080	100	Yes	5.850e-06	0.007
PG Static Pressure 11	[Pa]	101285.00	101284.16	101281.99	101285.00	100	Yes	3.01	6.63
PG Total Pressure 12	[Pa]	101333.61	101332.95	101330.28	101334.30	100	Yes	4.02	6.88
PG Dynamic Pressure 13	[Pa]	48.61	48.78	47.79	49.53	100	Yes	1.49	2.54
PG Velocity 14	[m/s]	8.905	8.926	8.829	9.000	100	Yes	0.114	0.215
PG Velocity (X) 15	[m/s]	0.213	0.213	0.120	0.292	100	Yes	0.049	0.093
PG Velocity (Y) 16	[m/s]	-0.065	-0.022	-0.096	0.122	100	Yes	0.043	0.043
PG Velocity (Z) 17	[m/s]	-8.856	-8.874	-8.945	-8.772	100	Yes	0.112	0.175
PG Turbulence Length 18	[m]	0.002	0.002	0.002	0.002	100	Yes	5.515e-05	1.713e-04
PG Turbulence Intensity 19	[%]	3.22	3.22	3.17	3.28	100	Yes	0.11	0.37
PG Turbulent Energy 20	[J/kg]	0.122	0.122	0.121	0.124	100	Yes	0.003	0.017

Inlet velocity	10.804	m/s
Outlet velocity	8.905	m/s
Turbulence intensity change	1.08	%
Average velocity change	1.899	m/s

The average velocity has a minor decrease; however, the flow itself exhibits instability due to oversized gaps and cell diameters.

4.4.7) 0.85 cm Octagonal honeycomb structure.

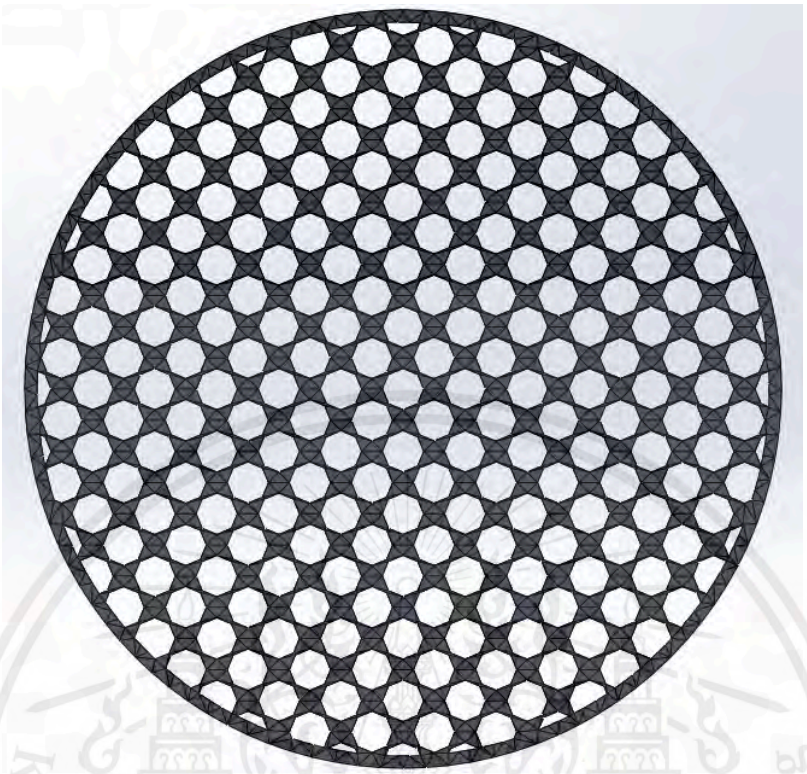

Figure 4.4.7.1

This design is intended to explore the impact of increased edge count on airflow. If the number of edges is a significant factor, this design should theoretically be more effective than the hexagon and other designs. The initial comparison reveals that the structural strength of this design is weaker compared to other shapes due to the unbalance and irrationality of each cell.

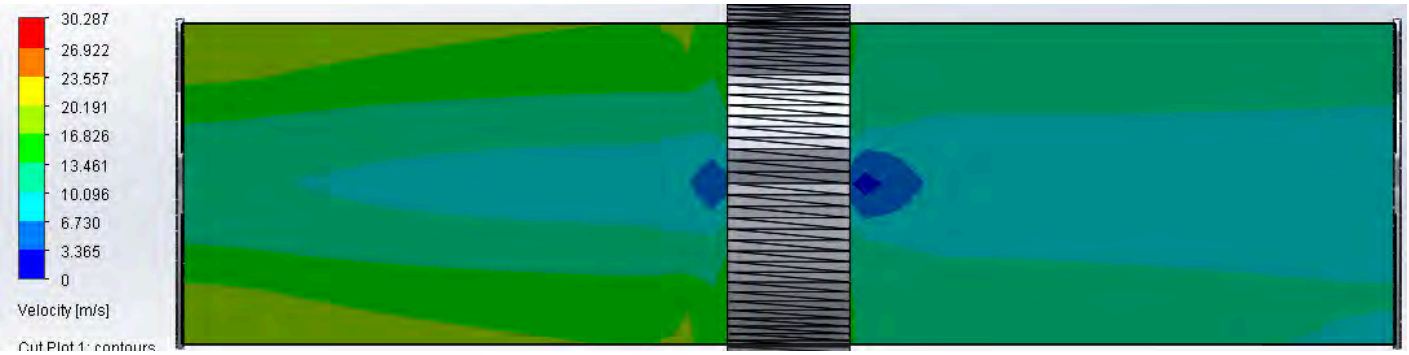

Figure 4.4.7.2 Velocity distribution

Goal Name	Unit	Value	Averaged Value	Minimum Value	Maximum Value	Progress [%]	Use In Convergence	Delta	Criteria
PG Static Pressure 1	[Pa]	101677.62	101677.80	101677.61	101678.04	100	Yes	0.43	278.70
PG Total Pressure 2	[Pa]	101744.58	101744.74	101744.57	101744.97	100	Yes	0.40	281.13
PG Dynamic Pressure 3	[Pa]	66.94	66.93	66.91	66.94	100	Yes	0.03	2.86
PG Velocity 4	[m/s]	10.502	10.501	10.500	10.502	100	Yes	0.002	0.241
PG Velocity (X) 5	[m/s]	-0.254	-0.254	-0.254	-0.254	100	Yes	1.744e-04	0.030
PG Velocity (Y) 6	[m/s]	0.056	0.056	0.056	0.056	100	Yes	4.825e-05	0.006
PG Velocity (Z) 7	[m/s]	-9.336	-9.336	-9.336	-9.335	100	Yes	0.002	0.369
PG Turbulence Length 8	[m]	0.002	0.002	0.002	0.002	100	Yes	2.569e-08	3.864e-05
PG Turbulence Intensity 9	[%]	2.23	2.23	2.23	2.23	100	Yes	3.72e-04	0.17
PG Turbulent Energy 10	[J/kg]	0.082	0.082	0.082	0.082	100	Yes	1.319e-05	0.008
PG Static Pressure 11	[Pa]	101323.58	101323.49	101323.39	101323.58	100	Yes	0.20	0.93
PG Total Pressure 12	[Pa]	101362.39	101362.25	101362.09	101362.42	100	Yes	0.33	4.77
PG Dynamic Pressure 13	[Pa]	38.80	38.76	38.66	38.84	100	Yes	0.18	4.06
PG Velocity 14	[m/s]	8.018	8.013	8.003	8.021	100	Yes	0.018	0.362
PG Velocity (X) 15	[m/s]	0.033	0.049	0.024	0.067	100	Yes	0.016	0.017
PG Velocity (Y) 16	[m/s]	-0.065	-0.069	-0.078	-0.061	100	Yes	0.014	0.021
PG Velocity (Z) 17	[m/s]	-7.983	-7.977	-7.985	-7.968	100	Yes	0.017	0.368
PG Turbulence Length 18	[m]	0.002	0.002	0.002	0.002	100	Yes	1.505e-05	1.058e-04
PG Turbulence Intensity 19	[%]	8.47	8.42	8.35	8.47	100	Yes	0.10	1.07
PG Turbulent Energy 20	[J/kg]	0.724	0.715	0.701	0.724	100	Yes	0.010	0.103

Inlet velocity	10.502	m/s
Outlet velocity	8.018	m/s
Turbulence intensity change	Increase 6.24	%
Average velocity change	decrease 2.484	m/s

After passing through the filter, the average velocity decreases, while turbulence intensity increases. Although the airflow tends toward laminar behavior, the velocity remains unstable. The distribution of air velocity fluctuates.

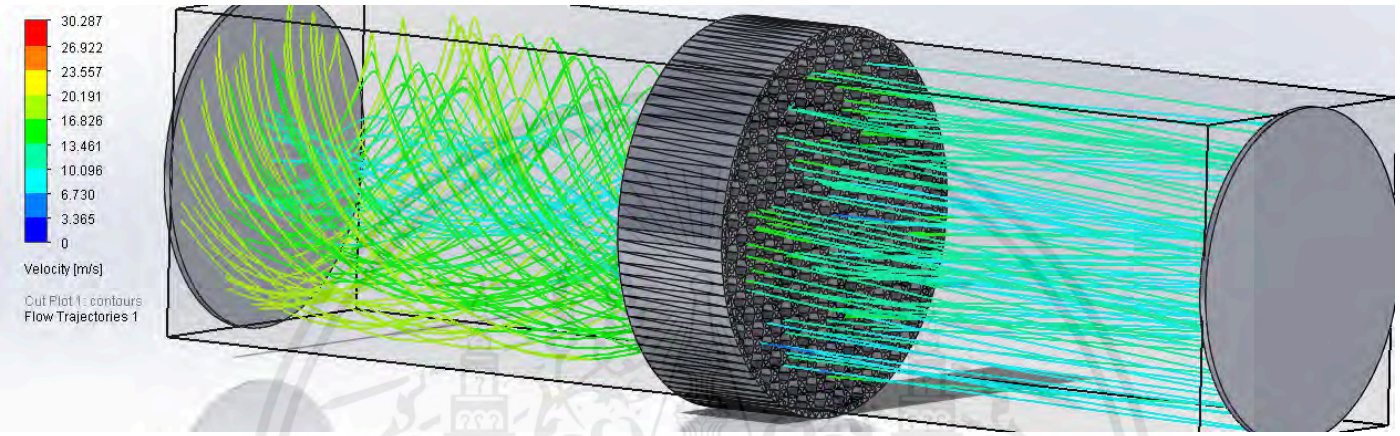

Figure 4.4.7.3 Flow trajectory

The flow trajectory of the octagon shape exhibits instability, with airflow velocity and direction showing deviations from a consistent laminar flow pattern. While there is a trend towards laminar behavior, the direction of airflow after passing through the structure fluctuates, indicating an unstable flow pattern.

4.4.8) 2.0 cm Octagonal honeycomb structure.

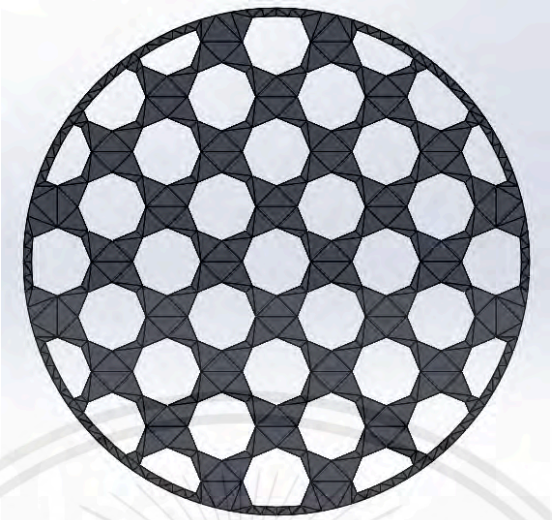

Figure 4.4.8.1

The 2.0 design of the Octagonal honeycomb pattern shares a similar issue with the 2.0 hexagonal pattern, which is the presence of large solid gaps between each cell. This structural characteristic is detrimental to airflow, impacting both velocity and turbulence distribution within the system.

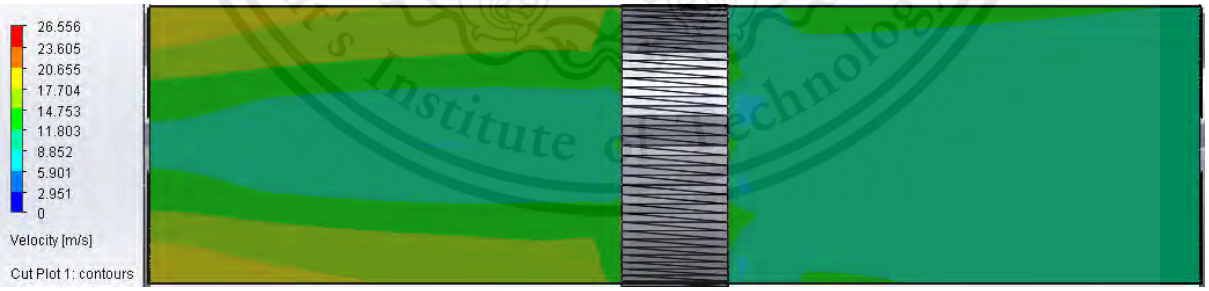

Figure 4.4.8.2 Velocity distribution

According to Figure 4.4.8.2, this design demonstrates favorable velocity distribution, with consistent velocities observed. Although there are minor fluctuations in velocity, the trend remains relatively stable. Additionally, turbulence flow tends to transition towards a laminar flow pattern after passing through the filter.

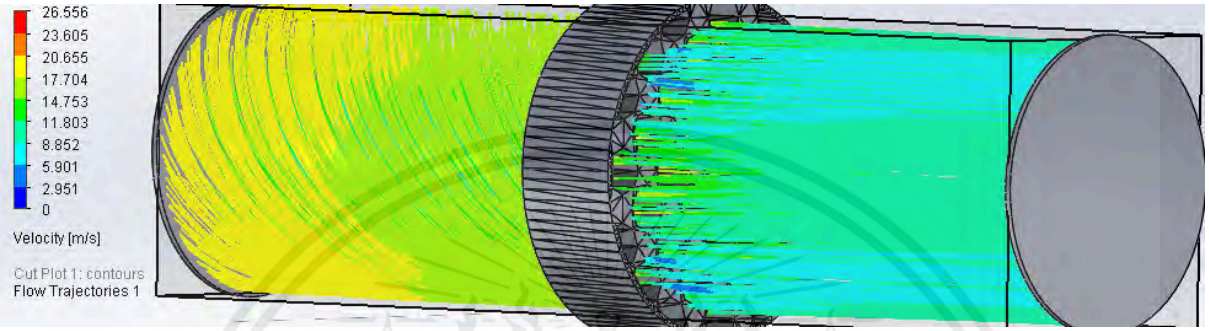

Figure 4.4.8.3 Flow trajectory

Summary

Goal Name	Unit	Value	Averaged Value	Minimum Value	Maximum Value	Progress [%]	Use In Convergence	Delta	Criteria
PG Static Pressure 1	[Pa]	101615.00	101615.53	101615.00	101615.97	100	Yes	0.52	79.46
PG Total Pressure 2	[Pa]	101679.21	101679.73	101679.21	101680.16	100	Yes	0.45	80.60
PG Dynamic Pressure 3	[Pa]	64.20	64.18	64.17	64.20	100	Yes	0.03	3.82
PG Velocity 4	[m/s]	10.298	10.297	10.296	10.298	100	Yes	0.003	0.327
PG Velocity (X) 5	[m/s]	-0.059	-0.059	-0.059	-0.059	100	Yes	1.258e-04	0.005
PG Velocity (Y) 6	[m/s]	-0.062	-0.062	-0.062	-0.062	100	Yes	8.627e-05	0.008
PG Velocity (Z) 7	[m/s]	-9.206	-9.205	-9.206	-9.204	100	Yes	0.002	0.454
PG Turbulence Length 8	[m]	0.002	0.002	0.002	0.002	100	Yes	3.572e-08	4.040e-05
PG Turbulence Intensity 9	[%]	2.27	2.27	2.27	2.27	100	Yes	4.68e-04	0.19
PG Turbulent Energy 10	[J/kg]	0.082	0.082	0.082	0.082	100	Yes	8.955e-06	0.008
PG Static Pressure 11	[Pa]	101313.39	101313.69	101313.39	101313.99	100	Yes	0.23	4.99
PG Total Pressure 12	[Pa]	101388.52	101388.51	101387.79	101389.07	100	Yes	0.33	2.98
PG Dynamic Pressure 13	[Pa]	75.11	74.81	74.19	75.34	100	Yes	0.55	3.57
PG Velocity 14	[m/s]	11.164	11.141	11.096	11.181	100	Yes	0.041	0.247
PG Velocity (X) 15	[m/s]	-0.042	-0.044	-0.134	0.025	100	Yes	0.027	0.029
PG Velocity (Y) 16	[m/s]	0.030	-0.010	-0.064	0.094	100	Yes	0.020	0.027
PG Velocity (Z) 17	[m/s]	-11.137	-11.117	-11.159	-11.073	100	Yes	0.041	0.246
PG Turbulence Length 18	[m]	0.002	0.002	0.002	0.002	100	Yes	2.034e-05	3.400e-05
PG Turbulence Intensity 19	[%]	3.56	3.57	3.53	3.60	100	Yes	0.04	0.36
PG Turbulent Energy 20	[J/kg]	0.240	0.240	0.236	0.243	100	Yes	0.003	0.032
Velocity Change	[m/s]	-0.866	-0.844	-0.883	-0.798	100	Yes	0.046	0.553

Inlet velocity	10.298	m/s
Outlet velocity	11.164	m/s
Turbulence intensity change	Increase 1.24	%
Average velocity change	Increase 0.866	m/s

The velocity on the surface of the 2.0 octagon honeycomb is slightly increased due to the presence of large solid gaps, which push the airflow towards the mesh cells. Despite turbulence intensity being within acceptable limits, this design is not commonly utilized in industrial settings due to its poor structural strength. Additionally, the higher cost of production further discourages its use.

4.5 Experiment

The aim of this project is to create and prepare a mount that would fit inside the wind tunnel connecting it to the Honeycomb filters with one side being fixed with the mount. By correctly measuring the mounts connecting the Honeycomb filters inside the wind tunnel, the mounts were fixed and fastened with the Honeycomb filter so that when the tests were conducted any leakage would be prevented. First off, we conducted a test where the Honeycomb filters weren't. Then, we conducted a test where we installed the different types of Honeycomb to be able to define which type of Honeycomb filter is the most efficient.

Figure 4.5.1

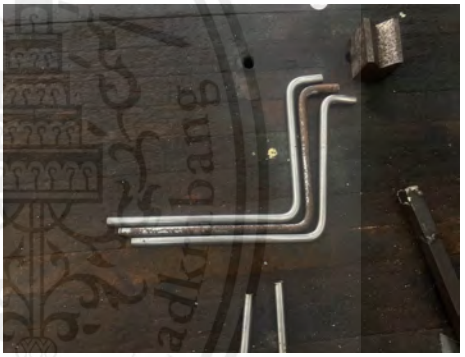

Figure 4.5.2

Figure 4.5.3

Figure 4.5.4

Figure 4.5.1 and Figure 4.5.2 as shown from the picture above are metal rods (12 mm) that are bent to be used as mounts to connect the Honeycomb filter into the Wind tunnel.

In figure 4.5.3 and Figure 4.5.4 is the drilling process where we used used a drill that is similar to the size of the rods (12 mm) in order for us to get the correct fit when attaching the rod to the Honeycomb filters

Figure 4.5.5

It is shown in this figure the finished product after successfully attaching the metal rod to the Honeycomb filters and ready for testing.

(Figure 4.5.6)

(Figure 4.5.6.1)

In this experimental setup, a Pitot tube meter (Figure 4.5.6) and air flow meter (Figure 4.5.6.1) are utilized to measure and display airflow characteristics. The recorded velocity data depicted in the figure represents the baseline velocity obtained without the inclusion of honeycomb filters in the wind tunnel. This baseline velocity serves as a crucial constant for reference and comparison throughout the experiment.

The constant number of Wind tunnels before inserting any honeycomb structure is 15.120 m/s. This number of air velocity can be considered and compared with the values we get after insert each filter.

Honeycomb Square

Figure 4.5.7

The model depicted in Figure 4.5.7 exemplifies the square honeycomb configuration, subjected to rigorous evaluation for wind velocity determination through the utilization of sophisticated instrumentation within a wind tunnel setting. This experimental setup incorporates state-of-the-art methodologies, employing both pitot tube meters and air flow tube meters to meticulously gauge the intricate dynamics of airflow within the controlled environment of the wind tunnel.

Velocity

Figure 4.5.8

The velocity obtained in this experiment for square honeycomb is 13.084 m/s by using wind tunnel and pitot tube meter. Comparing the velocity of when the Honeycomb square is less than the velocity of without having any filters.

Honeycomb Octagon

Figure 4.5.10

The model depicted in Figure 4.5.10 exemplifies the octagon honeycomb configuration, subjected to rigorous evaluation for wind velocity determination through the utilization of sophisticated instrumentation within a wind tunnel setting. This experimental setup incorporates state-of-the-art methodologies, employing both pitot tube meters and air flow tube meters to meticulously gauge the intricate dynamics of airflow within the controlled environment of the wind tunnel.

Velocity

Figure 4.5.11

Within the visual representation presented in Figure 4.5.11, it is discernible that the velocity recorded from the octagonal model conspicuously emerges as the least among the four distinct types of Honeycomb filters meticulously evaluated as part of our comprehensive testing protocol. Specifically, the velocity measurement attributed to this particular configuration is quantified at 12.043m/s, thereby elucidating its relatively subdued performance compared to its counterparts under scrutiny.

Honeycomb Circular

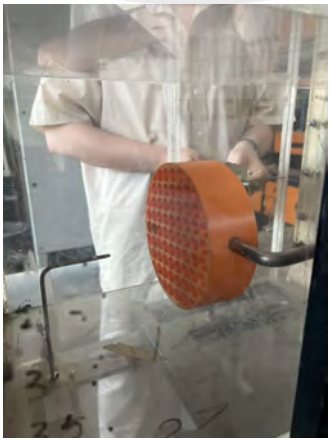

Figure 4.5.13

The model depicted in Figure 4.5.13 exemplifies the circular honeycomb configuration, subjected to rigorous evaluation for wind velocity determination through the utilization of sophisticated instrumentation within a wind tunnel setting. This experimental setup incorporates state-of-the-art methodologies, employing both pitot tube meters and air flow tube meters to meticulously gauge the intricate dynamics of airflow within the controlled environment of the wind tunnel

Velocity

Figure 4.5.14

The velocity obtained by using a pitot tube meter measured in the wind tunnel with a circular honeycomb model is 13.0128 m/s.

Honeycomb Hexagon

Figure 4.5.16

The model depicted in Figure 4.5.16 exemplifies the hexagon honeycomb configuration, subjected to rigorous evaluation for wind velocity determination through the utilization of sophisticated instrumentation within a wind tunnel setting. This experimental setup incorporates state-of-the-art methodologies, employing both pitot tube meters and air flow tube meters to meticulously gauge the intricate dynamics of airflow within the controlled environment of the wind tunnel

Velocity

Figure 4.5.17

The velocity obtained by using a pitot tube meter in the wind tunnel with the hexagon model is 12.257 m/s.

Normal velocity without the Honeycomb filters	15.120 m/s	
Velocity with Honeycomb Square	13.084 m/s	96
Velocity with Honeycomb Octagon	12.043 m/s	89
Velocity with Honeycomb Circular	13.028 m/s	109
Velocity with Honeycomb Hexagon	12.257 m/s	93

This table is the measurement of velocity from when Honeycombfilters weren't installed compared to the velocity when the Honeycomb filters were installed. For us to be able to obtain the values of velocity and pressure we used the device called the pilot tube meter, it is used to measure flowing velocity.

CHAPTER 5

CONCLUSION AND RECOMMENDATION

Result comparison

Design of Honeycomb	Change in Velocity	Change in Turbulence intensity
0.85 cm square honeycomb structure	+1.361 m/s	+1.34%
2.0 cm square honeycomb structure	- 2.224m/s	+0.66%
0.85 cm circular honeycomb structure.	-1.358 m/s	+5.69%
2.0 cm circular honeycomb structure.	+1.658m/s	+0.07%
0.85 cm Hexagon honeycomb structure.	+1.750m/s	-4.33%
2.0 cm Hexagon honeycomb structure	-1.899m/s	+1.08%
0.85 cm Octagonal honeycomb structure.	-2.484m/s	+6.24%
2.0 cm Octagonal honeycomb structure	+0.866m/s	+1.24%

Hexagonal grid patterns, such as those resembling honeycomb structures, offer certain advantages over other grid shapes when it comes to mitigating turbulence intensity in fluid flow simulations.

One key reason lies in the uniformity and regularity of hexagonal grids. Hexagons tessellate, meaning they can fill a plane with no gaps or overlaps, resulting in a more consistent distribution of grid cells compared to other shapes like squares or triangles. This regularity helps to reduce numerical errors and artifacts in the simulation, leading to more accurate representations of fluid flow phenomena.

Additionally, the arrangement of hexagonal cells inherently minimizes the presence of sharp corners or edges within the grid. This characteristic is significant because turbulence tends to amplify near geometric discontinuities, such as corners or edges, due to flow separation and vortex shedding. By minimizing these discontinuities, hexagonal grids can help to mitigate turbulence intensity and improve the overall stability of the simulation.

Moreover, hexagonal grids often exhibit better isotropy, meaning that the grid spacing is more uniform in all directions. This isotropic nature ensures a more balanced representation of turbulence characteristics across different flow directions, contributing to more accurate predictions of turbulence intensity.

Overall, the regularity, reduced presence of sharp edges, and improved isotropy of hexagonal grids make them advantageous for capturing fluid flow phenomena with lower turbulence intensity compared to other grid shapes.

REFERENCES

[1] Gonsalves, D. C. (2019). Design and analysis of an open circuit subsonic wind tunnel. Retrieved from https://pubs.aip.org/aip/acp/article-abstract/2080/1/040005/688705/Design-and-analysis-of-an-open-circuit-subsonic?redirectedFrom=PDF

[2] Cody , S. (2022). Mit unveils New Wright Brothers wind tunnel. Retrieved from https://news.mit.edu/2022/mit-unveils-new-wright-brothers-wind-tunnel-0608

[3] Glove, D. (2021). Comparison of hexagonal, square, and circular sections. Retrieved from https://dergipark.org.tr/tr/download/article-file/2060998

[4] Spahn, J. (2020). How to build and use a subsonic wind tunnel. Retrieved from https://www.sciencebuddies.org/science-fair-projects/references/how-to-build-a-wind-tunnel

[5] Hix, K. D. (2020). Experimental evaluation of a honeycomb structure in open ... Retrieved from https://scholarsmine.mst.edu/cgi/viewcontent.cgi?article=8955&context=masters_theses

[6] Samardzic, A. (2016). Design of unsteady wind tunnel. Retrieved from https://core.ac.uk/download/pdf/212995166.pdf

[7] Scheima, J. (1981). Considerations for the installation of honeycomb ... Retrieved from https://ntrs.nasa.gov/api/citations/19810020599/downloads/19810020599.pdf

[8] TE Automotive-AABE. (n.d.). Wind tunnels used in aerodynamics. Retrieved from https://www.gcoeara.ac.in/learning_material/auto/TE/Automotive Aerodynamics/Unit -3a wind tunnel.pdf

[9] Hamzah, H. (2021). Role of honeycomb in improving subsonic wind tunnel ... Retrieved from https://jmerd.net/Paper/Vol.44,No.7(2021)/352-369.pdf

[10] Manshadi, M. D. (2011). The importance of turbulence reduction in assessment of wind tunnel flow quality. Retrieved from https://www.intechopen.com/chapters/16897